Vegdirektoratet
Trafikksikkerhet, miljø- og teknologiavdelingen
Tunnel og betong
Desember 2016

Statens vegvesen

Internt sulfatangrep i sprøytebetong med perlitt

Etatsprogrammet Varige konstruksjonar 2012-2015

STATENS VEGVESENS RAPPORTAR Nr. 582

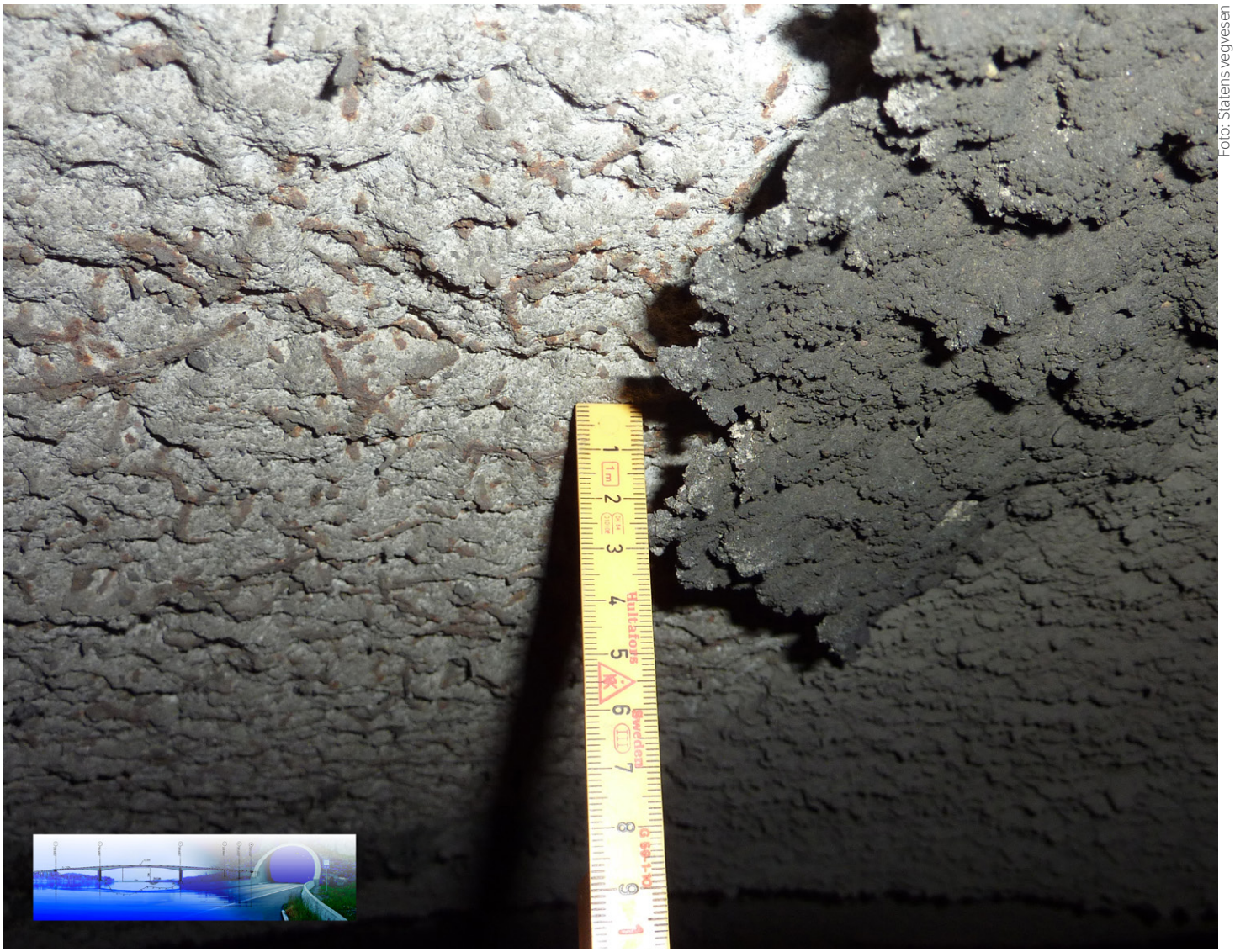

Foto: Statens vegvesen

Tittel
Internt sulfatangrep i sprøytebetong med perlitt

Undertittel
E16 Nes tunnelen

Forfattar
Per Hagelia

Avdeling
Trafikksikkerhet, miljø- og teknologiavdelingen

Seksjon
Tunnel og betong

Prosjektnummer
603242

Rapportnummer
Nr. 582

Prosjektleiar
Synnøve A. Myren / Alf Kveen

Godkjent av
Synnøve A. Myren

Emneord
Varige konstruksjoner, tilstandsutvikling tunnel, sprøytebetong, perlitt, internt sulfatangrep

Samandrag
Nestunnelen på E16 blei stengt i nesten tre år på grunn av avskaling og nedfall av sprøytebetong med ekstrudert perlitt brukt til brannsikring av polyetylen (PE)-skum. Årsakene til betongskadane var omfattande utluting av sementlimet, karbonatisering, destruktiv stålfiberkorrosjon, intern sprenging av natriumsulfat kombinert med fukt, frost og dynamiske laster frå trafikk. Den omfattande utlutinga tyder på tidleg syreangrep. Undersøkinga viste at perlitt i dette tilfelle må ha inneheldt SO_2-gass som gav opphav til svovelsyre. Natrium frå vannglas-akselerator og oppløyst perlitt reagerte med sulfat og gav opphav til natriumsulfat.

Title
Internal sulfate attack in sprayed perlite concrete

Subtitle
E16 Nes tunnel

Author
Per Hagelia

Department
Traffic Safety, Environment and Technology Department

Section
Tunnel and concrete

Project number
603242

Report number
No. 582

Project manager
Synnøve A. Myren / Alf Kveen

Approved by
Synnøve A. Myren

Key words
Durable structures, existing tunnels, sprayed concrete, perlite, internal sulfate attack

Summary
The Nes tunnel on expressway E16 was closed for nearly three years due to extensive spalling and fallout of sprayed concrete made with extruded perlite used for fire protection of polyethylene foam panels for water and frost protection. The concrete damage was caused by decalcification of the cement paste matrix, carbonation, destructive steel fiber corrosion and expansion of sodium sulfate in combination with moisture, freeze/thaw and dynamic loads from traffic. The extensive decalcification indicates early sulfate attack. The investigation suggests that the perlite pores contained SO_2-gas, which gåve rise to sulfuric acid. Sodium from water glass setting accelerator and dissolved perlite glass reacted with sulfate, leading to formation of sodium sulfate.

Tal sider 30
Dato Desember 2016

Pages 30
Date December 2016

Forord

Denne rapporten inngår i en serie rapporter fra **etatsprogrammet Varige konstruksjoner**. Programmet hører til under Trafikksikkerhet-, miljø- og teknologiavdelingen i Statens vegvesen, Vegdirektoratet, og foregår i perioden 2012-2015. Hensikten med programmet er å legge til rette for at riktige materialer og produkter brukes på riktig måte i Statens vegvesen sine konstruksjoner, med hovedvekt på bruer og tunneler.

Formålet med programmet er å bidra til mer forutsigbarhet i drift- og vedlikeholdsfasen for konstruksjonene. Dette vil igjen føre til lavere kostnader. Programmet vil også bidra til å øke bevisstheten og kunnskapen om materialer og løsninger, både i Statens vegvesen og i bransjen for øvrig.

For å realisere dette formålet skal programmet bidra til at aktuelle håndbøker i Statens vegvesen oppdateres med tanke på riktig bruk av materialer, sørge for økt kunnskap om miljøpåkjenninger og nedbrytningsmekanismer for bruer og tunneler, og gi konkrete forslag til valg av materialer og løsninger for bruer og tunneler.

Varige konstruksjoner består, i tillegg til et overordnet implementeringsprosjekt, av fire prosjekter:

Prosjekt 1: Tilstandsutvikling bruer
Prosjekt 2: Tilstandsutvikling tunneler
Prosjekt 3: Fremtidens bruer
Prosjekt 4: Fremtidens tunneler

Varige konstruksjoner ledes av Synnøve A. Myren. Mer informasjon om prosjektet finnes på vegvesen.no/varigekonstruksjoner

Denne rapporten tilhører **Prosjekt 2: Tilstandsutvikling tunneler** som ledes av Alf Kveen. Prosjektet vil skaffe kunnskap om den tekniske tilstanden på tunnelers konstruksjon og utrustning og øke kunnskapen om nedbrytningsmekanismer. Formålet med prosjektet er å utvikle bedre verktøy for tilstandsutvikling, noe som er viktig både for planlegging av drift og vedlikehold av eksisterende tunneler. Prosjektet vil også etablere kunnskap som kan bidra til at fremtidige tunneler bygges og innredes slik at ønsket kvalitet og levetid oppnås.

Rapporten er utarbeidet av *Per Hagelia*, Statens vegvesen

Innhald

1 Innleiing

Betongskader fører i blant til omfattande reparasjonsarbeider med behov for stenging av vegtunnelar. Det er alltid ein fordel å avdekke skadeårsakene, fordi dette gir viktig informasjon om både eksponeringsforhold og riktig materialval.

Nestunnelen på E16 blei stengt frå mars 2011 til februar 2014 på grunn av omfattande avskaling og nedfall av sprøytebetong brukt som brannsikring av PE-skum. Med utgangspunkt i denne uvanlege hendinga og svært lange stengingsperioden valte Etatsprogrammet Varige konstruksjonar å undersøkte skadeårsakene nærmare.

Denne rapporten gir ei oppsummering av undersøkinga. Den detaljerte dokumentasjonen er gitt i ein fagartikkel som blei publisert i Proceedings of the 15th Euroseminar on Microscopy Applied to Building Materials – Delft, Nederland i 2015 (Hagelia 2015; Vedlegg 1).

2 Undersøking av perlittbetong og mikro-PP fiber brukt som brannsikring i Nestunnelen – E16

2.1 Historikk og feltdokumentasjon

Nestunnelen er 1276 m lang og blei opna i 1988. Vass- og frostsikringskvelv med polyetylen (PE-) skum blei montert. Omkring 1988-1989 var det eit stort fokus på brannsikring av PE-skum, og ein valde å sikre PE-skummet med stålfiberarmert lettbetong (Robotic 10) med tilslag av ekstrudert perlitt og sand. Etter omkring 10 år blei det oppdaga skader på perlittbetongen fleire stader.

Ekstrudert perlitt er eit svært porøst materiale som er basert på ein porøs vulkansk bergart (perlitt) med kjemisk samansetning tilsvarande silisium-rik rhyolitt (granittisk kjemi). Vulkansk gassar, bl.a. vatn og svoveldioksid, er alltid er til stades frå naturen si side. Oppvarming til omkring 850-900 °C fører til at bergarten blir mjuk og ekspanderer svært kraftig på grunn av gassporetrykk. Ein reknar gjerne med at det er vatnet i den vulkanske gassen som er hovudårsaka til ekspansjonen, og at all gass slepper ut. På den andre sida er naturleg perlitt ekstremt viskøs i oppvarma tilstand, og det er derfor lite sannsynleg at all vulkansk gass blir frigjort. Dersom ein i framstilling av ekstrudert perlitt også nyttar kol eller olje i oppvarming vil det venteleg også kunne tilførast komponentar, sannsynlegvis også svovel i form av svoveldioksid. Ekstrudert perlitt har svært god isolerande effekt og er blant anna brukt som lett tilslag til betong.

Detaljert inspeksjon i 2002 avdekte horisontale og vertikale sprekker i brannsikringa med behov for reparasjon. Skadane var bare delvis knytta til lekkasjar gjennom vass- og frostsikringskvelvet. Ein fann også 500 kg laus bergmasse på ein stad bakom vass- og frostsikringskvelvet.

Reparasjonane i 2002 omfatta forsegling av opne sprekker med PE-skum, samt mindre lekkasjeførande sprekker med silikon. Deretter blei det sprøyta opp ny stålfiberarmert lettbetong med ekstrudert perlitt. For å forsterke konstruksjonen ytterlegare blei det utanpå perlittbetongen sprøyta opp eit ca. 4 cm tjukt lag av sprøytebetong med brannbestandig mikro-PP fiber. Til slutt blei det påført omkring 3 cm med fiberfri «ordinær» sprøytebetong på den nedste meteren over vegbanen (Figur 1). Reseptar og andre detaljar er oppgitt i Vedlegg 1.

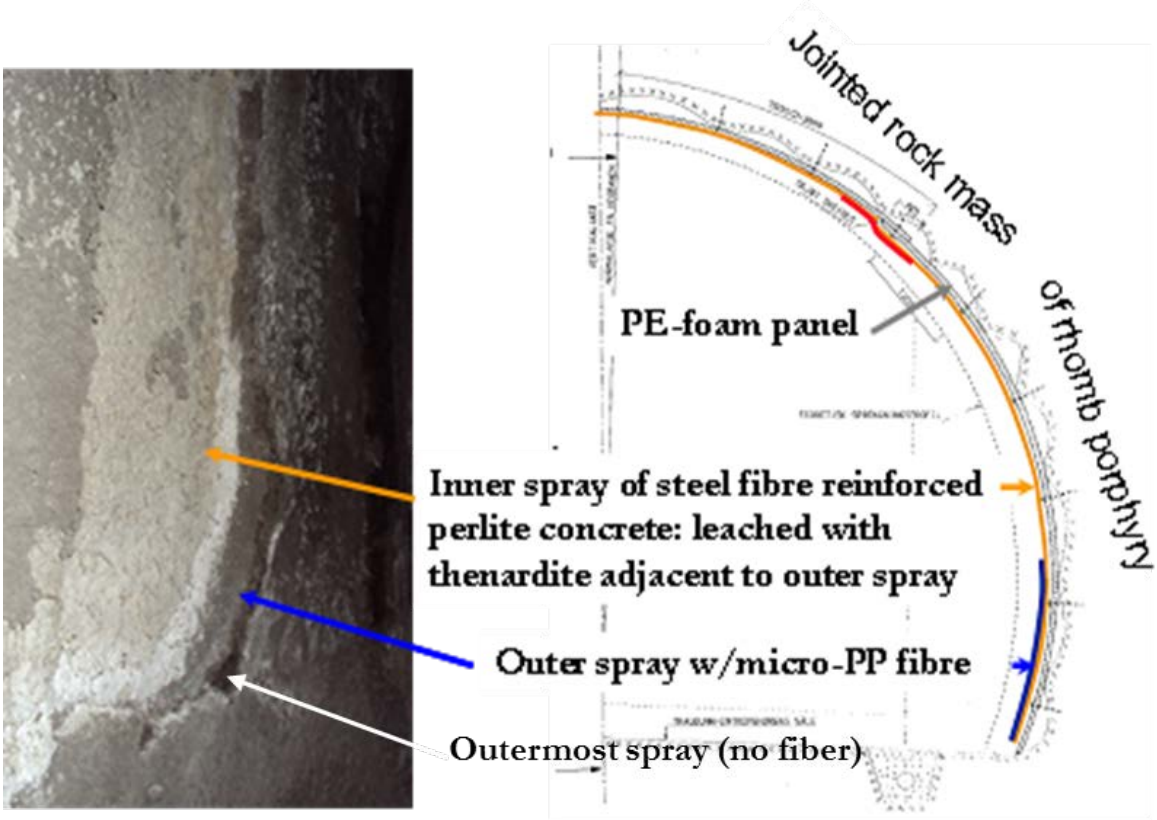

Figur 1 Tverrsnitt gjennom skadd brannsikring i 2011 (frå innerst til ytterst): 1) Lys grå stålfiberarmert sprøytebetong med ekstrudert perlitt mot PE-skum; var sprø og svak på grunn av kraftig karbonatisering og delvis gjennomrusta stålfiber, 2) Kvit sone i perlittbetongen med natriumsulfat (thenarditt), delvis som kvitt pulver, 3) Grå ytre sprøytebetong med mikro-PP fiber. 4) Ytre lag av fiberfri sprøytebetong; bare i nedste delar ca. I m over vegbana (Hagelia 2015).

Reparasjonane i 2002 blei kontrollerte både under og etter sluttført arbeid, og det blei rapportert at dei var vellykka og utført med høg kvalitet. Resultatet er vist i Figur 2.

Etter omkring ni år var det observert avskaling, og tidleg på morgonen den 3. mars 2011 falt det ned omkring 200 kg sprøytebetong (Figur 3og Figur 4). Ein bil blei skadd, og tunnelen blei stengt med det same. Det viste seg at avskalinga av sprøytebetongen var utvikla over mestedelen av tunnelen, og i mykje større omfang enn det som var synleg ved overflateinspeksjon. Avskalinga hadde tydeleg samanheng med svært omfattande karbonatisering og frostbelastning. Sannsynlegvis var avskalinga også påverka av dynamiske laster frå vegtrafikken (Holm 2011). Dette støttast også av målte trykk og sugkrefter på nokså tilsvarande konstruksjonar (Davik 1994).

Figur 2 Nestunnelen rett etter reparasjon i 2002. Ny sprøytebetong med perlitt blei påført, saman med eit ytre lag av mikro-PP fiber betong utan perlitt. Fiberfri sprøytebetong blei til slutt sprøyta opp på den nedste meteren over vegbanen. Foto: Statens vegvesen.

Figur 3 Nestunnelen i 2011, ni år etter reparasjon. Det var kraftig avskaling i heile tunnelen med nedfall og skade på bil. PE-skummet var blottlagd fleire stader. Foto: Statens vegvesen.

Figur 4 Situasjon etter at vass- og frostsikringskvelvet var rive ned. Det var relativt tørt i tunnelen, men med lokale fuktgjennomslag. Kvit og pulverisert perlittbetong ligg på vegbanen saman med restar av PE-skum. Foto: Statens vegvesen.

2.2 Geologi og vatn

Nestunnelen går gjennom rombeporfyr-lava. Denne bergarten er rik på feltspat og inneheld ikkje skadelege mineral, så som svovelkis eller tilsvarande reaktive sulfidmineral.

Tunnelen var for tørr for å samle inn vassprøve, men på ein plass bak vass- og frostsikringskvelvet var det utfelt eit kvitt stoff på bergmasse av rombeporfyr omkring ein tidlegare lekkasjesprekk. Dette blei undersøkt mineralogisk ved røntgendiffraksjon (XRD), og viste seg å vere karbonatmineralet thermonatritt $Na_2CO_3 \cdot H_2O$. Ein kunne dermed slå fast at grunnvatnet ikkje fører sulfat. Karbonatet vitnar i tillegg om at pH-verdien til grunnvatnet ikkje kan ligge på den sure sida av skalaen.

2.3 Utluting av sementpasta, karbonatisering og natriumsulfat

Det blei samla inn eit utval betongprøver frå tunnelen i april 2011, før reparasjonsarbeida starta opp. Vi valte ut typiske prøver av variabelt svekka betong, inklusive betongflak med typisk kraftig karbonatisering og destruktiv stålfiberkorrosjon, fragment av kvitt nedbrytingsprodukt til dels som pulver (Figur 5), samt mikro-PP betong. Det blei ikkje samla inn prøver av den ytre/nedre fiberfrie betongen, som verka å vere intakt.

Det blei laga tynnslip av to betongflak, N1 og N2 av hhv perlittbetong og betong med ytre mikro-PP fiberbetong. Desse blei undersøkte både i polariasjonsmikroskop og Scanning elektronmikroskop (SEM). Fragment av ulike variantar blei valt ut for SEM og

røntgendiffraksjon (XRD). Ei prøve av kvitt pulver, Nes-1, frå ytre område av perlittbetong mot mikro-PP betong, og betongflak N1 blei også analysert med tanke på svovelisotopsamansetning.

Tynnslipa viste at det ikkje var svovelkis, magnetkis eller andre sulfidmineral i dei naturlege tilslagsmateriala, verken i perlittbetongen eller betongen med mikro-PP fiber. Sementpastaen i *perlittbetongen* var porøs og kraftig utluta mht. kalsium (Ca). Portlanditt ($CaOH_2$) var fråverande, og kalsium-silikat-hydrat (C-S-H) var også utarma med tanke på Ca. Kalsium frå utluta pasta hadde reagert med karbonation og var utfelt som sekundært kalsiumkarbonat spreidd omkring mellom tilslagskorna (såkalla Popcorn kalsitt, Figur 6).

Utlutinga hadde gitt ei *svært lys gul-gulbrun farge på pastaen* og ført til kraftig stålfiberkorrosjon med utfelling av store brune rustflekker i sementpastaen omkring alle fibrar. Rusta hadde trekt inn i den porøse sementpastaen, utan tydeleg sprengande verknad. Dette viser at oppløyste Fe^{2+} ion må ha blitt transportert inn i matriks og først deretter utfelt som rust ved oksidasjon til treverdig jern. Den kraftige Ca-utlutinga frå sementpastaen kombinert med utfelling av Popcorn kalsitt og rustimpregnering av porøs sementpasta tyder på rask og omfattande senking av gjennomsnitts pasta pH, frå >13 ned til ca. 8 i eit oksiderande miljø. Utfelling av rust (treverdig jern) føregår ved pH > 4.5 ved tilgang på oksygen. Samstundes vil oppløyst Fe^{2+} bare vere muleg ved pH < 4.5 noko som tyder på lokale pH-variasjonar i samband med fiberkorrosjonen. Figur 7 viser at utfelling av korrosjonsprodukta er mest omfattande i kontakt med perlitt, delvis med utfelling inni perlittporer. Samla sett er dette tydelege teikn på syreangrep, med klare indikasjonar på at syra var knytta til ekstrudert perlitt.

Mikro-PP betongen utanpå var derimot stort sett intakt med typisk mørk og tett pasta, bortsett frå nokre område ved kontaktsona mot perlittbetong. *Det var tydeleg at skadeårsaka var lokalisert til den underliggande perlittbetongen.*

Røntgenopptaka viste at kvit og pulverisert betong stort sett bestod av natriumsulfat i form av mineralet thenarditt (Na_2SO_4). Sjølv om dette sulfatet også finst i sement, var mengda i dette tilfellet ekstremt høg. Vi ser ikkje elles natriumsulfat i røntgenopptak av normalt hydratisert sementpasta. Dette var uventa, særleg fordi det kvite pulveraktige laget blei funnen overalt mellom perlittbetong og ytre betong, og ikkje bare der lekkasjevatn og luft hadde slept til via sprekker og fuger i vass- og frostsikringskvelvet. Dette understreker også at sulfatangrepet var internt.

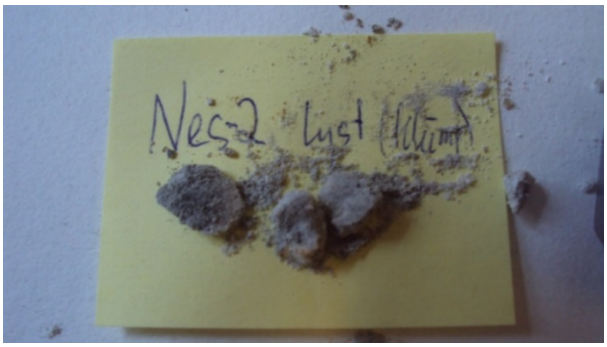

Figur 5 Kontaktsona mellom sprøytebetong med perlitt og sprøytebetong med mikro-PP fiber inneheld stort sett kvitt natriumsulfat (thenarditt) i form av pulver og svakt materiale. Foto: Per Hagelia.

SEM-analysar viste at perlitt-tilslaget delvis var kollapsa (Figur 6). Dette må ha skjedd under sprøyteoperasjonen. I områder der perlittilslaget var intakte var det tydeleg at poreveggane av glas var svært tynne (Figur 7). I Vedlegg 1 er det referert til forsking som viser at syklisk utfelling og oppløysing av thenarditt har større sprengande verknad enn vekslande hydratisering og dehydratisering av natriumsulfat.

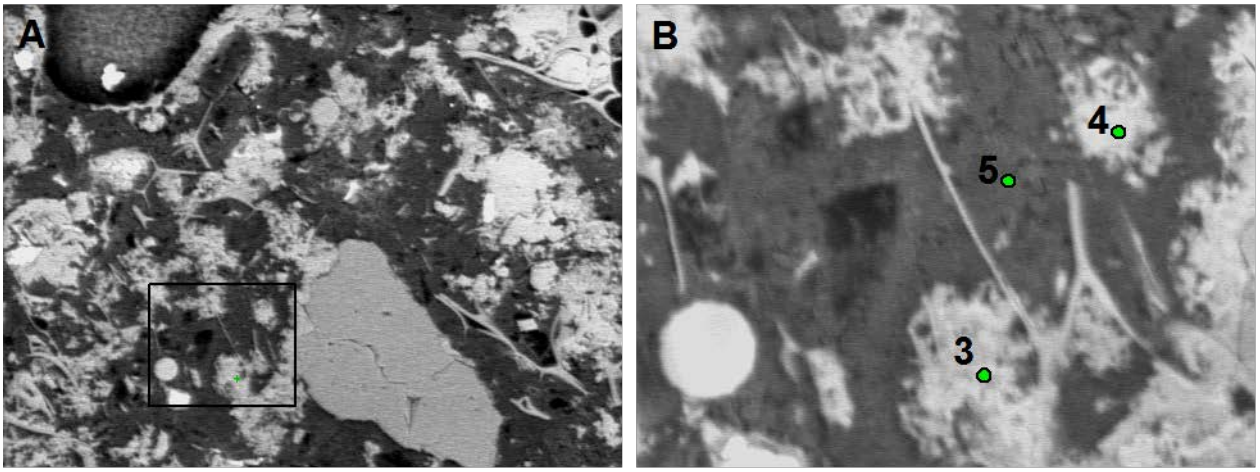

Figur 6 Delvis kollaps av perlitt sett i Scanning elektronmikroskop. Dei tynne strengane er perlittglas. Mørk grått er sterkt utluta sementpasta. Kvite område er kalsiumkarbonat utfelt i pasta («Popcorn kalsitt»), som også inneheldt litt svovel. Også eit tilslagskorn av kvarts (lys grått i venstre bilde). Foto: Naturhistorisk Museum.

Mikrokjemiske analysar viste at både pasta og utfelt kalsiumkarbonat (Popcorn kalsitt) alltid inneheld litt svovel, noko som ein elles ikkje ser i karbonatisert betong (detaljar i Vedlegg 1).

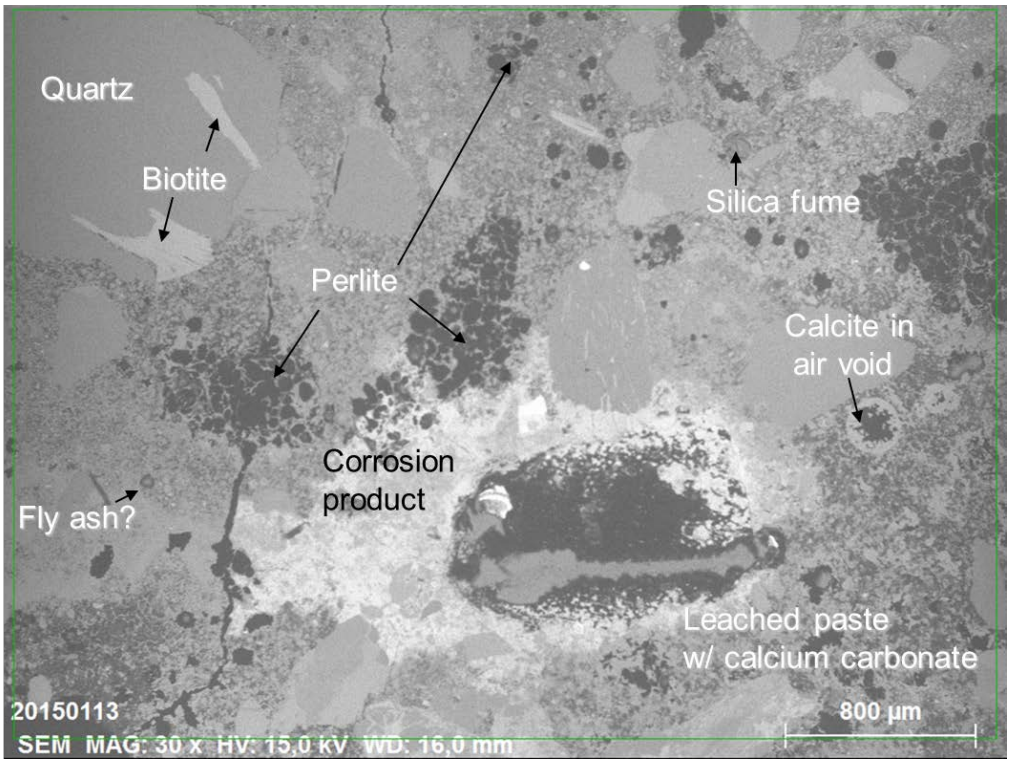

Figur 7 Intakt perlitt sett i Scanning elektronmikroskop. Sementpastaen var også her sterkt utluta og karbonatisert. Korrosjonsprodukt (rust) viste ingen sprengande verknad, men var utfelt/trekt inn i sementpastaen omkring sterkt korrodert stålfiber og var nært knytta til perlitt og (lyst område). Også flygeaske og udispergert silika blei identifisert. Foto: Naturhistorisk Museum.

2.4 Svovelisotopar avdekker kor svovelet kjem frå

Svovelisotopar blir brukt blant anna for å skille mellom ulike typar svovelkjelder. Slike undersøkingar har etter kvart blitt vanlege i miljøstudiar, men er også brukt for å avdekke årsaker til nedbryting av bygningsmaterialar (sjå bl.a. Sanjurjo-Sanchez & Alves 2012).

Prøver av perlittbetong blei analyserte for $\delta^{34}S$, som er eit forholdstal mellom dei to viktigaste svovelisotopane ^{32}S og ^{34}S. $\delta^{34}S$ uttrykkast i promille i forhold til ein internasjonal standard (sjå Vedlegg 1). S-isotopsignaturen gir ofte tilstrekkeleg informasjon om kor svovelet kjem frå, men kan også seie noko om kjemiske prosessar som er involvert.

Gips som tilsettast sementklinker kjem frå gammalt inndampa havvatn. Fordi svovelisotop-samansetninga ($\delta^{34}S$) i havet har endra seg over geologisk tid (Figur 8: Claypool et al. 1980) er det muleg å bruke svovelisotopar for å avgrense opphavet til råmaterialet. Svovel frå forbrenning av olje og kol har andre verdiar, og er ofte anrika i ^{32}S.

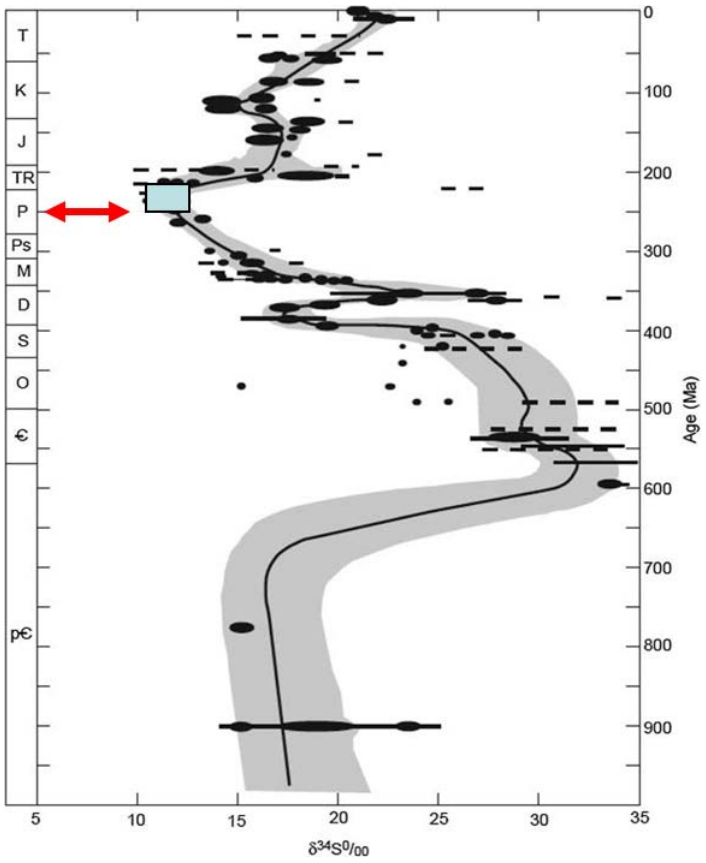

Figur 8 Gips tilsett sementklinker kjem frå gammalt inndampa havvatn. Svovelisotop- samansetninga (δ34S) i havet har endra seg over geologisk tid (Claypool et al. 1980). Den røde pila viser δ34S verdiane i perlittbetongen, og kan ikkje forklarast ut frå kjent variasjon i råmaterialet for tilsett gips, men er ei blanding av sement-gips og svært sannsynleg SO2 tilført frå gass i perlitt.

Analysar av svak perlittbetong frå Nestunnelen gav verdiar for $\delta^{34}S$ frå +5.73 ‰ til +9.19 ‰. Pulver av natriumsulfat (mineralet thenarditt) låg midt mellom med $\delta^{34}S$ = 7.44 ‰. *Desse verdiane er signifikant lågare enn alle tenkbare råmateriale for gips tilsett sement*.

Tidlegare undersøkingar av upåverka C-S-H i sprøytebetong gav $\delta^{34}S$ = +10.6 ‰ for Åkebergveien (betongalder 1987) og $\delta^{34}S$ = +11.8 ‰ i Svartdalstunnelen (betongalder 1998-1999) (Iden & Hagelia 2003). Med utgangpunkt i desse verdiane er det sannsynleg at norsk sement omkring 1987-88 var tilsett gips med opphav frå Zechstein gips, som er av yngre Permisk alder (P, i Figur 8). Alternativt kan også gips frå Tertiær (TR) ha vore råmaterialet ($\delta^{34}S \approx$ +10 ‰ til + 22 ‰), eller kanskje også frå Devon (D). Ein analyse av norsk sement frå 2000 gav derimot $\delta^{34}S$ = +21.3 ‰. Dette kan tyde på endring i gips-råstoff omkring tusenårsskiftet, eller at ein brukte fleire leverandørar.

Gips ($CaSO_4 \cdot 2H_2O$) er alltid tilsett Portland klinker. Dei låge verdiane frå perlittbetongen i Nestunnelen må tolkast som ei blanding av gips ($\delta^{34}S \geq$ +11-12 ‰), og ein komponent med lågare isotopverdiar enn perlittbetongen (dvs. $\delta^{34}S <$ +5.73 ‰). Det er vanskeleg å tenke seg andre komponentar med slike verdiar enn SO_2 (eller evt. H_2S). Råmaterialet for ekstrudert perlitt er den vulkansk bergarten perlitt. SO_2 er ein vanleg vulkansk gass og i tillegg er det

ikkje usannsynleg at ein i framstillinga av ekstrudert perlitt kan ha brukt eit svovelholdig fossilt brennstoff. Gjennomsnittleg svovelisotopsamansetninga for SO_2 frå fossilt brennstoff i Europa har $\delta^{34}S \approx 4$ til 5 ‰ (Institutt for energiteknikk 2002). Vulkansk SO_2 ligg ofte nær dette, men kan også ha lågare verdiar. Også bileksos vil ofte ha liknande låge verdiar.

Det faktum at porevolumet i perlitt i stor grad hadde kollapsa under sprøyteoperasjonen, viser at gass i perlitt må ha sleppt ut omtrent samtidig som betongen begynte å herde. Vidare har intakt perlittglas svært tynne vegger. Perlitt er eit svært alkalireaktivt materiale, og tynne porevegger vil derfor lett løysast opp i kontakt med ordinær sementpasta, som har svært høg pH (Mladenović m. fl. 2004). Det er derfor sannsynleg at stadig nye gassfylte porer vil opne seg over tid. Svovelisotopane tyder sterkt på at perlittgassen førte SO_2.

SO_2 frigjort frå perlitt reagerte dermed med vatn og danne svovelsyre; både tidleg (kollapsa under sprøyteoperasjonen som førte til lokalt tidleg syreangrep) og litt etter litt i område med normal høg pH verdi ved oppløysing av perlitt (suksessiv senking av pH). Også eventuell H_2S-gass vil reagere med oksygen og danne svovelsyre. Det er nødvendig å vurdere om SO_2 frå eksos kan vere årsaka til den lette isotopsignaturen, men det er usannsynleg at eksos kan ha påverka betongen, fordi:

- Ein eventuell påverknad frå svovel i eksos ville vere mest tydeleg i dei ytre betonglaga. Dette er ikkje i samsvar med at svovel og natriumsulfat er avgrensa til djupare nivå, omkring 4–5 cm under overflata mot tunnelrommet.
- Sprøytebetongen i Nestunnelen blei laga med v/b = 0.42–0.47, og sementpastaen burde uansett ikkje i utgangspunktet ha høg gasspermeabilitet. Den ytre meir ordinære betongen, med mikro-PP fiber utan lett tilslag, ville dessutan beskytte underlaget.
- Nestunnelen var normalt godt utlufta og har i tillegg pipe-effekt.
- Effektar av same type nedbryting burde vere vanleg i mange tunnelar, og særleg i tunnelar med høgare trafikk enn i Nestunnelen. Tvert imot er det ikkje dokumentert at normal vegtrafikk kan føre til kraftig sulfatangrep.

Også i dei undersjøiske Ellingsøy- og Valderøy tunnelane (Ålesund) har det tidlegare blitt dokumentert store problem med bestandigheit av perlittbetong brukt som brannsikring. Rapportar frå Strømme (1994), Noteby (1997) og SINTEF (1990) viser at også her var perlittbetongen svært sterkt karbonatisert og svekka etter mindre enn ti år, og med kraftig stålfiberkorrosjon og utfelt rust i pastavolumet. Desse rapportane dokumenterte også kloridinntrenging, men at dette ikkje såg ut til å forklare årsaka til den kraftige fiberkorrosjonen. Den sterke graden av stålfiberkorrosjon blei knytta til omfattande karbonatisering. Det er ikkje usannsynleg at skadeårsaka i Ålesundstunnelane var den same som i Nestunnelen.

Alle nemnte tunnelar er nå rehabiliterte. Det er i staden brukt mikro-PP i brannsikringa.

3 Oppsummering av reaksjonsmekanismar

Undersøkingane i Nestunnelen viste at årsaka til nedfall var nært knytta til internt sulfatangrep. Ein konkluderer med følgjande skademekanisme (Vedlegg 1):

- Under sprøyteoperasjonen blei det porøse perlittilslaget delvis knust (kollapsa) og sleppte ut SO_2 frå poregassen.
- SO_2 reagerte med vatn til svovelsyre, noko som førte til utluting av Ca frå sementpastaen og dermed hindra normal hydratisering av klinkerminerala.
- Det blei sannsynlegvis også danna syre over lenger tid ved at SO_2 slapp ut litt etter litt frå meir intakt perlitt, på grunn av svært tynne poreveggar. Perlittglas er ikkje stabilt i kontakt med porevatn i betong.
- Dette gir ei forklaring på at det var unormalt høgt svovel både i sementpastaen og i sekundært utfelte karbonat.
- Ca frigjort ved utluting reagerte med CO_2 til kalsiumkarbonat ($CaCO_3$) i form av «Popcorn kalsitt» i sementpastaen, utfelling på luftporer, samt finkorna karbonatisering.
- Angrepa førte til destruktiv stålfiberkorrosjon, utan tydeleg sprengande effekt frå korrosjonsprodukta.
- Sekundær gips blei ikkje danna i syreangrepet, fordi all kalsium blei bunde i kalsiumkarbonat.
- Natrium frå vannglas akselerator reagerte med gjenverande sulfat og danna natriumsulfat, særleg nær kontaktsona mot den ytre sprøytebetongen med mikro-PP fiber. Natrium blei sannsynlegvis også tilført over tid, ved opplysing av perlittglas i (mikro-)områder med gjenverande høg pH. Tinesalt kan i tillegg ha tilført natrium i nedre delar av sprøytebetongen.
- Varierande uttørking og oppfukting, samt fryse-tine syklar, førte til at natriumsulfat blei vekselvis oppløyst og utfelt og på den måten fekk ein sprengande verknad som førte til avskaling.
- Dynamiske laster frå trafikken med trykk og sugkrefter førte til at relativt tynn og svak sprøytebetong blei ytterlegare svekka.

Takkens ord

Takk til Synnøve Myren for oversikt over problemstillinga, hjelp i tunnelen og arbeid med å skaffe fram eldre dokumentasjon. Hedda Vikan skal ha takk for kritiske kommentarar i gjennomlesinga av den norske teksten (sjå også «Acknowledgements» i artikkelen).

4 Referansar

Claypool,GE, Holster, WT, Kaplanm IR, Sakai, H & Zak, I (1980): The age curve of sufur and oxygen isotopes in marine sulfate and their mutual interpretation. Chemical Geology, 28, 199-260.

Davik, KI (1994): Metoder for vann- og frostsikring av vegtunneler, Delprosjekt B: Trykkimpulser fra vogntog i vegtunneler. Internrapport 1727. Vegdirektoratet, Veglaboratoriet.

Davik, KI (1997): Riktig bruk av sprøytebetong i tunneler. Brannsikring av PE-skum. Statens vegvesen, 33 sider.

Hagelia, P (2015): Spalling of sprayed perlite concrete caused by popcorn calcite deposition and internally derived sodium sulfate under influence of water leakage, frost action and synamic loads. 15th Euroseminar on Microscopy Applied to Building Materials, Delft, The Netherlands, s387-400.

Holm, J.V. (2011): E16 Nestunnelen – nedfall av sprøytebetong. Norconsult - Notat nr.1, Oppdragsnr. 5111160

Iden, KI & Hagelia, P (2003): C, O and S isotopic signatures in concretes which have suffered thaumasite formation and limited thaumasite form of sulfate attack. Cement and Concrete Composites, 25, 839-846.

Institutt for energiteknikk (2002): Prosjekt OPS E18 Nørholm – Timenes. Sulfidførende gneis og forsuring – bruk av isotoper for sporing av kilder.

Mladenović, A, Šuput, JS, Dicman, V. & Škapin, AS (2004). Alkali-silica reactivity of some frequently used lightweight aggregates. Cement and Concrete Research 34, 1809-1816.

Noteby (1997): Statens vegvesen Vegdirektoratet. Laboratorieanalyse av lett sprøytebetong, Robotic 10, som brannsikring av PE-skum. Valderøytunnelen og Ellingsøytunnelen. Noteby Rapport 68281-1.

Sanjurjo-Sanchez, J & Alves, C (2012). Pollutant-induced decay of building materials.

E.Lichtfouse, J Schwartzbauer, D Roberts (Eds): Environmental Chemistry for a Sustainable World. Volume 2: Remediation of Air and Water Pollution, pp 47-120.

SINTEF (1990): Undersøkelse av sprøytebetong fra undersjøiske vegtunneler. Skjølsvold, O og Jensen, V SINTEF-FCB, Rapport STF65 F90058, 81 sider

Strømme, OL (1994): Miljøskader på perlittbetongen i Ellingsøytunnelen. Statens vegvesen Møre og Romsdal. Hovudarkiv: 45.658, Oppdrag: Nr 94.007. Lab.arkiv RV 658 HP 1

Vedlegg 1 Dokumentasjon av Nestunnelen.

Hagelia (2015): Spalling of sprayed perlite concrete caused by popcorn calcite deposition and internally derived sodium sulfate under influence of water leakage, frost action and dynamic loads.

Spalling of sprayed perlite concrete caused by popcorn calcite deposition and internally derived sodium sulfate under influence of water leakage, frost action and dynamic loads

Per Hagelia

Norwegian Public Roads Administration, TMT, Tunnel and Concrete Division

per.hagelia@vegvesen.no

Abstract

A Norwegian road tunnel opened for traffic in 1988 was closed in 2011 due to severe spalling of light weight sprayed concrete. Initially a 2-3 cm thick layer of steel fiber reinforced sprayed concrete with extruded perlite aggregate was employed for fire protection of polyethylene (PE-) foam panels used for water and frost protection. Repair work in 2002 involved spraying of some new perlite concrete and a ca 40 mm thick outer layer of fire resistant sprayed concrete with micro-polypropylene (micro-PP) fiber. Petrography, SEM and XRD in 2011 showed that the spalling zone, being located around the interface between the two concrete layers, contained mainly thenardite. Also the adjacent micro-PP fiber concrete was partly influenced. Mirabilite was not detected, whilst minor amounts of a thaumasite-like phase was occasionally present. The entire layer of perlite concrete was very friable and had suffered destructive steel fiber corrosion. This was characterised by extensive carbonation, internal sulfurised Popcorn calcite deposition (PCD) and severe Ca-depletion of the cement paste matrix, hence resembling some features of acid attack. Spalling was particularly well developed where water had seeped through the PE-foam plates and affected by freeze/thaw. The tunnel is located within a Permian rhomb-porphyry lava sequence with no external sulfate source, and the concrete sand aggregate was devoid of sulfur-bearing minerals. However, stable S isotopic signatures ($\delta^{34}S$) imply that perlite aggregate contributed sulfuric acid: The S isotopes in thenardite, sulfurised carbonate and acid leached residue were lighter than common cement gypsum sources. Variable moisture and temperature conditions, frost action and dynamic loads from the traffic provided a favourable environment for micro cracking, ion migration, precipitation /dissolution and combined action of thenardite and pore-ice.

Keywords: Sprayed concrete, internal sulfate attack, thenardite, carbonation, frost action

I. Introduction

Sprayed concrete is used in Norwegian road tunnels for rock mass reinforcement in conjunction with rock bolts and as fire protection of polyethylene (PE) foam panels used for water and frost protection. Degradation of tunnel concrete is not a general problem. However, steel reinforced sprayed concrete for rock support has suffered some slow degradation in the Alum shale environment, due to Thaumasite Sulfate Attack (TSA) with associated popcorn calcite depositiom (Hagelia et al. 2001, 2003). Also a spotwise significant sprayed concrete deterioration caused by combined bacterial and abiotic attack occurs in some subsea tunnels, leading to localised thinning where Mn and Fe-rich biofilms are acting simultaneously with Ca-leaching, popcorn calcite deposition, TSA and Mg attack (Hagelia 2007, 2013). In general thicker layers of sprayed concrete are more durable than relatively thin layers (Davik 1998, Hagelia 2011). In contrast, degradation of sprayed concrete used for fire protection is apparently uncommon, although mechanically induced fracturing has been observed in some tunnels (Norwegian Public Roads Adminsitration 1997, Davik 1998).

This paper reports on a severe attack within sprayed concrete used for fire protection of PE-foam panels in a road tunnel in East Norway. This unusual incident, involving sprayed concrete with light weight perlite-aggregate, had caused severe spalling and closure of the tunnel for nearly three years.

History of concrete degradation in the Nes road tunnel and main technical data

The Nes road tunnel on expressway E16 in East Norway was opened for traffic in 1988. The tunnel is 1276 m long, serving about 11000 vehicles every day. Steel fiber reinforced concrete and rock bolts were used for rock mass reinforcement, whilst PE-foam panels were installed as an inner lining for water and frost protection. Due to the inflammable properties the PE- panels were fire-protected by a 2-3 cm thick layer of steel fiber reinforced light-weight sprayed concrete, containing very porous extruded perlite and sand aggregates. After about ten years in service some damage was discovered within the perlite sprayed concrete at several places. A detailed inspection was undertaken in 2002, unraveling need for reparations. Loose rock mass amounting to about 500 kg was also discovered at one location behind the water panel. The damage in perlite sprayed concrete was characterised by horizontal and vertical penetrative cracks, several of which carried water leakages. Reparations in 2002 involved sealing of wide cracks with PE-foam, whilst smaller cracks with water leakages were sealed with silicon. Thereafter the cracks were sprayed by new steel fiber reinforced perlite concrete. A special adhesive was applied for making the concrete stick to the PE-panels. In order to further strengthen the light-weight sprayed concrete a ca. 4 cm thick layer of concrete with micro-PP fiber was sprayed in the lower parts of the tunnel profile along the entire tunnel length, reaching about one meter above the road level. The micro-PP fibers concrete was subsequently covered by a ca. 3 cm thick spray of fiber-free "ordinary" sprayed concrete (Figure 1%2).

In the early morning on March 3rd, 2011 about 200 kg of sprayed concrete fell down, and one vehicle was damaged. The tunnel was immediately closed for traffic, at first for a thorough inspection. The conclusion after inspection was that the tunnel should be closed on permanent basis and that complete refurbishment would be the most feasible solution. The tunnel was not reopened for traffic until February 2014.

The 1988 sprayed perlite concrete (Robotic 10) was made with Portland cement, silica fume and steel fiber reinforcement. The cement was most likely CEM I. Water glass was used as setting accelerator. However, the water/binder ratio and other details have not been reported. In 2002 thorough water cleaning of the entire tunnel was undertaken prior to reparation. The new concrete mixes are presented in Table 1. According to internal documents at NPRA the work was thoroughly controlled during and after it was finished, showing good and satisfactory workmanship.

Inspections in 2011 by NPRA and Norconsult showed that spalling of the perlite concrete was developed throughout most of the tunnel. It was not possible to differentiate visually between damaged and undamaged areas, because hammering unraveled a much wider extent of spalling than was obvious through superficial inspection. Observations clearly indicated that the spalling involved frost action and carbonation, likely assisted by vibrations due to dynamic air pressure induced by vehicles (Holm 2011). However, no laboratory analysis and microscopy were applied.

Objectives

Due to the severe implications of the concrete degradation it was decided to undertake a more detailed investigation, with the clear aim of diagnosing the deterioration mechanism and its causes. The objectives of this work were to:

- Present the main tunnel observations and sampling of degraded sprayed concrete
- Characterise and diagnose the degradation mechanisms by the aid of concrete petrography, X-ray diffraction and Scanning electron microscop (SEM) analysis
- Investigate the ultimate source of aggressives involved, assisted by stable S isotope analysis
- Discuss the spalling mechanism

II. Methods in the field and laboratory

Field methods

Samples were collected in April 2011 after the tunnel was closed. Spalls and smaller samples of degraded concrete were collected from different layers along with degradation products located at the interface between perlite concrete and outer micro PP-fiber concrete. Spall samples were collected in plastic bags and sealed and debris samples were put into small glassed with tight plastic lids. All samples were essentially dry.

Laboratory methods

The analytical work is summarised in Table 2. The thin sections were investigated under a standard polarising microscope and analysed by SEM. Debris samples and chips of friable concrete were analysed by X-ray diffraction (XRD) and Scanning Electron Microscopy (SEM). Stable S-isotopes were analysed in two samples.

Preparation of thin sections. Two concrete spalls, approximately two cm thick, were cut at right angle across layering with a diamond saw and washed thoroughly. Standard polished thin sections without fluorescent dye were prepared on 27 mm x 45

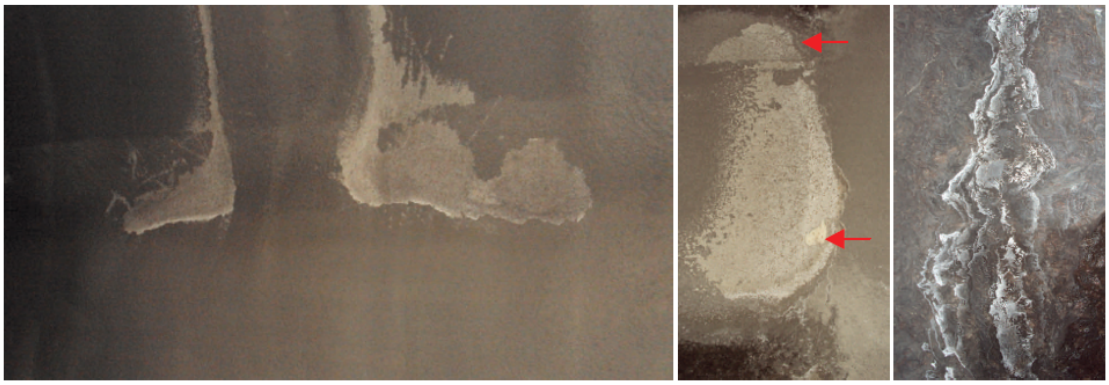

Figure 1: Left: *Well developed spalling in the 1988 sprayed concrete, terminating about 1 m above the road. Apparently the wider lower spalls had also developed in the upper parts of the 2002 sprayed layers.* Middle: *Severe spalling in 1988 and 2002 sprayed concrete, being typically developed within the perlite layer: Previous spalling in 1988 perlite concrete (upper arrow) is partly covered by 2002 sprayed concrete, displaying extensive and more recent spalling with exposed PE-foam panel (lower arrow)* Right: *Bright white thermonatrite efflorescence deposited from ground water on rhomb porphyry rock mass (widths of photos; about 3 m; 1 m & 0.8 m, respectively).*

mm glass slides, representing perlite concrete and outer sprayed concrete with micro-PP fiber. Water was used as coolant; hence possible presence of soluble phases such as thenardite were not preserved in the thin sections.

Polarising microscopy. The thin sections were studied under a standard polarising microscope with objectives 5x, 10x, 20x and 50 x. Domains with degradation products and other features were identified, several of which were further analysed by SEM.

X-ray diffraction (XRD). Small samples about 0.5-2 grams were handpicked from debris and friable concrete under a stereomicroscope at 20-50x magnification and ground in small agate mortars under ethanol. The samples were left to dry in air at ambient laboratory temperature, mounted on sample holders and run in a Siemens D 5000 Spectrometer. All diffractograms were recorded from 2^o to 70^o on the 2-Theta scale at 0.050^o per second. The spectrometer was set to 40 kV and 40 nA using Ni-filtered CuKα radiation with wavelength (λ) = 1.54178 Å. The diffractograms were checked versus the Powder Diffraction Files database from the International Centre for Diffraction Data. Mineral proportions are regarded as qualitative to semi-quantitative.

Scanning electron microscopy (SEM). Thin sections and concrete debris and other friable samples were analysed. This involved point analysis (1-2 μm^2) and X-ray element mapping. All samples were mounted on carbon tape without coating. A Hitachi 3600N scanning electron microscope with an EDS unit from Thermo Electronic Corporation was used. The instrument was operated with an accelerated voltage of 15 kV and 10 Pa vacuum. Analytical precision for major elements is within 1-2 wt.% for spot analysis on thin sections and other even surfaces. The analytical work was undertaken soon after collection and preparation in 2011, thus avoiding aging. However, X-ray mapping and two points were analysed in thin section N2 in January.

Sulfur isotopes. Sulfur in thenardite-rich powder (Nes 1) was obtained by homogenization of the

*Table 1: Concrete mixes in the Nes road tunnel. Weights of cement, aggregate and perlite are given in units of 1 m^3 of concrete; Sand grading 0-4 mm; Cylinder strength. *) = No data; **) = SF by cement weight.*

Perlite concrete 1988	Perlite concrete 2002	PP-fiber concrete 2002	"Ordinary" concrete
Portland cement, *	Portland cement * = 450 kg	Portland cement * = 465 kg	Portland cement * = 465 kg
Silica fume*	Silica fume = 20 kg**	Silica fume = 30 kg**	Silica fume = 30 kg**
Water glass	Water glass	Water glass	Water glass
Fine sand*	Sand = 550 kg	Sand = 1580 kg	Sand = 1577 kg
Perlite*	Perlite = 1450 kg		
Steel fiber	Steel fiber = 1 kg	Micro-PP fiber	Fiber free
w/c*	w/b = 0.47**	w/b = 0.42**	w/b = 0.42**
	Strength = 13-22 MPa	Strength $\approx$ 35 MPa	Strength = 31-37 MPa
	ρ= 1500-1850 kg/m^3	$\rho\approx$2225 kg/m^3	ρ= 2211-2260 kg/m^3

sample, followed by direct combustion of the sample in presence of V_2O_5. Three equal samples were prepared in tin capsules. The extensively carbonated concrete sample N1 was first crushed to a fine powder in an agate mortar. From this bulk material three equal samples were packaged into tin capsules in the presence of V_2O_5. The remaining material was washed in 2N HCl to release S bound to calcite and other soluble phases, and subsequently washed with deionised water, dried, and three equal samples were packaged into tin capsules in the presence of V_2O_5. The sample capsules were combusted at 1700 ^oC and reduced to SO_2, which was analysed in a Nu Horizon isotope mass spectrometer along with IAEA standard NBS 127 and Elemental Microanalysis standard B2308 (quantification reference). Isotopic composition and S concentration were analysed in the same instrument. The analytical precision in $\delta^{34}S$ is $\pm$ 0.2 ‰(1 σ) and the isotopic values are given relative to the Canyon Diablo troilite standard.

III. Results

Field observations and sampling

The sprayed concrete was severely spalling in most parts of the tunnel, being developed in a spot-wise fashion in the ceiling and tunnel walls. The sizes of spalled areas varied from a few square decimeters to more than one square meter, whilst the spall thicknesses were about 0.5 to 2.5 centimeter. The spalling was at several places developed as vertical long and narrow zones connected to wider spalls in the lower parts of the tunnel walls. Yet the sprayed concrete below about 1 m above the road level, corresponding to 2002 repair concrete, had not developed much visible spalling (Figure 1). However, also the 2002 perlite concrete was spalling (Figures 1 & 2).

The vertical narrow spalls were sometimes related to joints in the PE-foam panels behind, and were possibly also governed by previous penetrative cracks in the 1988 concrete. Although the tunnel concrete was essentially dry to at the time of sampling, there was clear evidence for Ca-leaching, suggesting that water and frost must have had a profound impact. Indeed, the fire protected PE-foam panels were installed along the entire length of the tunnel due to the presence of widespread moisture and water seepages in the tunnel in 1988. The local climate is characterised by cold winters, rainy seasons and variably hot summers.

Spalling was controlled by a weak very light-colored layer, in most cases located in the outer parts of the perlite concrete. The spalling zone was frequently characterised by presence of a white powder representing totally disintegrated concrete. The PE-foam panels were exposed at several locations (Figure 1). It was otherwise evident that the perlite concretes had suffered extensive carbonation with severe and mainly destructive steel fiber corrosion all over the place. Also the adjacent parts of the outer micro-PP fiber concrete were in part cracked and friable. The features of the concrete attack were essentially the same everywhere.

Spalls and debris samples were collected from each sprayed concrete layer at suitable locations within the middle parts of the tunnel. In most cases the samples could be broken loose without using a hammer. In general it was not easy to differentiate between the two generations of perlite concrete. No water leakage was available for proper water sampling. Consequently the chemical nature of ground water load could not be directly established. However, at one location bright white surface efflorescence sitting on barren rock mass was reached (Figure 2). It was hoped that its composition might shed light on the ground water chemistry from which it had been precipitated. A white efflorescence was also collected from the southern portal.

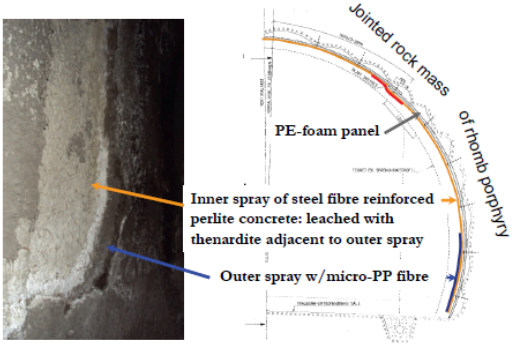

Figure 2: Cross section showing three layers of sprayed concrete: 1) inner light colored 1988 perlite concrete with internal spalling due to extensive carbonation and destructive steel fiber corrosion, followed by 2002 concrete; 2) grey sprayed concrete with micro-PP fibers and 3) outer dark sprayed concrete without fibers. Breath of photo is about 50 cm.

XRD

XRD analysis was performed on perlite concrete, associated degradation products and white efflorescence material both from barren rock (Figure 1) and the tunnel portal. The results from XRD analysis are summarised in Table 3. In general, quartz and feldspar represents aggregate minerals. Calcite in degraded and friable perlite concrete represents extensive carbonation of the cement paste. "Possible minors" were indicated by very minor peaks, but were not rigorously proven.

Sodium sulfate was always present in the white

Table 2: Summary of analytical work on sprayed concrete samples from the Nes road tunnel.

Sample No./characteristics/type of material	Polarising microscopy	XRD	SEM	S- isotopes
Nes-1 White powder in perlite concrete at interface w/PP concrete		X	X	X
Nes-2 White very friable perlite concrete		X	X	
Nes-3 Grey friable mico-PPfiber concrete			X	
Nes-4 White powder at interface w/PP-concrete		X		
Nes pr 1 Efflorescence on rhomb porphyry rock mass		X		
Nes pr 2 White powder at interface w/PP-concrete		X		
Nes pr 3 Efflorescence from crack in tunnel portal		X		
N-1 Perlite concrete w/corroded steel fiber	X		X	X
N-2 Perlite concrete & outer PP-concrete	X		X	

to light colored powder samples. Nes-1 consisted of thenardite and a little quartz. Nes-4 contained quartz, calcite and lesser amounts of thernardite, with a possible very minor amount of vaterite. Nes pr. 2 was particularly interesting in that two forms of sodium sulfate occurred. Thenardite, being face-centered orthorhombic Na_2SO_4 (*form V*) and base-centered orthorhombic sodium sulfate (*form III*) occurred together with quartz and a little calcite. Portlandite and gypsum were possibly present. Mirabilite ($Na_2SO_4{\cdot}10H_2O$) was not detected.

Sample Nes-2 of white and very strongly degraded perlite concrete contained much thenardite and also Ca-mordenite ($CaAl_2Si_{10}O_{24}{\cdot}7H_2O$), which is a zeolite. XRD analysis of Nes-2 also indicated presence of a silicon oxide ($Si_{100}O_{200}$). This substance is known mainly as a molecular sieve. Its occurrence in degraded perlite concrete remains obscure, but it seems possible that this silicon oxide may be related extruded perlite or silica fume.

Sample Nes pr 1 of white efflorescence sitting on the rhomb porphyry rock mass behind the PE-foam panel (Figure 1) contained thermonatrite ($Na_2CO_3(H_2O)$) with lesser amounts of quartz and anorthite. There was no evidence of sulfur bearing phases. Hence, it seems very unlikely that ground water in the area is enriched in sulfate. Sample Nes pr 3 of white efflorescence precipitated on a penetrative crack in one of the tunnel portals (cast concrete) consisted mainly of pure calcite, yet with possible traces of portlandite and gypsum. This likely represents leaching of the concrete.

Petrography - polarising microscopy

Thin section N1 of extensively carbonated sprayed perlite concrete was characterised by a light brown-yellowish cement paste matrix when viewed in plane polarised light. The paste was extensively leached, with isotropic character in crossed polars. The carbonation was represented by ubiquitous Popcorn calcite deposition (PCD) with individual calcite grains typically about 20-50 μm. However, also much finer carbonation had occurred, resembling features of ordinary carbonation. Calcite was also deposited in some air voids and locally within the pore space of perlite. Portlandite was apparently absent. Only few suspect grains of unhydrated cement were observed within the Ca-depleted cement paste matrix. Some undispersed brown silica fume globules, about 50-150 μm big, were found scattered about in the matrix. Also, dark brown, transparent and glass-like spheres about 20-50 μm big were found, probably representing fly ash agglomerations.

Rusty iron-rich deposits occurred, which had also led to a brown staining of the adjacent cement paste matrix. No steel fiber were preserved in the thin section, however, holes in the middle of some dense rust deposits suggested that less corroded steel had

*Table 3: Summary of XRD results on degraded concrete from the Nes road tunnel. Two structural forms of Na_2SO_4 were identified; thenardite (form V) and sodium sulfate * (form III).*

Samples	XRD minerals	Possible minors
Nes-1/white powder	Thenardite > quartz	
Nes-2/white friable fragment	Thenardite > mordenite $\gg$ quartz > silicon oxide	
Nes-4/white powder	Quartz > calcite > thenardite	Vaterite?
Nes pr 1/efflorescense on rock mass	Thermonatrite > quartz $\approx$ anorthite	
Nes pr 2/white powder	Thenardite > sodium sulfate* > quartz > calcite	Portlandite? Gypsum?
Nes pr 3/efflorescence from crack in tunnel portal	Calcite $\gg$ quartz	Portlandite? Gypsum?

been lost during thin section preparation.

The perlite aggregate particles were ranging in sizes from about 50 to 1000 μm and were extremely porous. Suspect thin glass shards of perlite were also observed scattered about in the cement paste matrix, which was confirmed in SEM. The remaining aggregate consisted of granitic rocks including micro-granite, siltstone and single grains of plagioclase, quartz, biotite and amphibole. The aggregate particles were rounded to angular with D_{max} about 5 mm. Opaque minerals were mainly Fe-Ti-oxides. Inspection in reflected light, using an external light source, showed that sulfide minerals were absent.

Thin section N2 included both sprayed perlite concrete and outer micro-PP fiber sprayed concrete. The perlite concrete here was sharing the same characteristics as sample N1. In contrast, the cement paste matrix in the outer sprayed concrete with micro-PP fiber was dark brown in plane polarized light, and did not appear to be much leached. The contact region adjacent to perlite concrete was, however, somewhat porous, with some large entrapment voids (reaching 300 μm). In a small domain next to an entrapment void apparent thaumasite had replaced cement paste, showing typical straw yellow color in plane polarised light and grey first order birefringence in cross polarised light. However, the SEM work showed this to be a little more complex.

The aggregate in outer concrete consisted of granitic rocks, siltstone, limestone, mica-gneiss, quartzite, and single grains of quartz, feldspars, amphibole and biotite. The aggregate particles were otherwise similar in shape and grading as in the sprayed perlite concrete. In a single micro-domain a gel-like isotropic material was found forming a thin rim inside an air void.

Scanning electron microscopy, micro-analysis and X-ray mapping

The SEM analysis was performed on the thin sections and several small debris samples. Analytical data from these two sample types must be regarded as complimentary. Sodium sulfate is soluble and not expected to have been preserved during thin sections preparation, which involved water cooling. Moreover, additional SEM work on samples analysed by XRD might shed further light on their composition, because of the possibility of mixed or amorphous phases.

Perlite concrete in thin sections N1 and N2. Figure 3 shows a typical micro domain of perlite concrete in *sample N2*. The image is from outer perlite concrete few mm beneath the micro-PP fiber concrete and may represent the 2002 spray. Severe carbonation here had caused destructive steel fiber corrosion. The mineral aggregate was quartz-rich with no sign of sulfides. The cement paste matrix was characterised by extensively developed PCD and finer grained carbonates. The initial calcium silicate hydrate (CSH) was completely degraded due to Ca-leaching, and the matrix was very friable and porous with variably penetrative micro-cracks. Undispersed silica fume lumps (100-200 μm) and suspect fly ash spheres (20-50 μm) were observed.

The results of X-ray element mapping are shown in Figure 4. The element distribution shows that Ca, O and lower intensities of C occupy the same domains in the paste. This reflects the presence of calcium carbonate, which was also Mg-substituted especially in the upper right parts of the analysed frame. However, the highest intensities of carbon represent epoxy in highly porous perlite, air voids and micro-cracks. The iron stained paste is clearly indicated by high Fe intensity. It is noteworthy that S was mainly occurring in the cement paste matrix, whilst the lower intensities of Na and Cl were scattered about without any particular relation to phase boundaries observed in back scatter. Most likely the latter feature reflects presence of soluble de-icing salt being smeared out on the thin section surface as a result of preparation. The mineral aggregate particles were clearly indicated by the higher intensities of Si, Al, K, Na and Ti. Perlite was not well indicated on this map, being overshadowed by other phases.

An important observation was that a very significant amount of the pore space of extruded *perlite had in fact collapsed*. Strings and shards of perlite glass occurred scattered about everywhere, being well embedded within depleted cement paste matrix with PCD (Figure 5). These textural relations clearly suggest that collapse must be a primary feature, e.g. that partial perlite collapse has taken place already during the spraying operation.

Micro-PP fiber concrete in thin section N2. SEM imaging confirmed that this outer concrete was sounder than the perlite concrete. The cement paste was often characterised by a normal looking cement paste matrix without PCD and other obvious signs of extensive moisture transport and Ca-depletion. However, the surface region was very porous and inhomogeneous, with occasional big lumps of undispersed silica fume, as seen in Figure 6C. The thaumasite like material (Figure 6B), located in a small micro domain about 200 μm away from perlite concrete, had replaced local cement paste, hence resembling features of a localised Thaumasite sulfate attack (TSA). However, chemical analysis showed that this is not a typical thaumasite but rather a very carbonate rich thaumasite-ettringite like phase (see details below). This mineral occurred in presence of a large entrapment void, and had also formed a faint fringe deposit inside this void. The entrapment void was joined

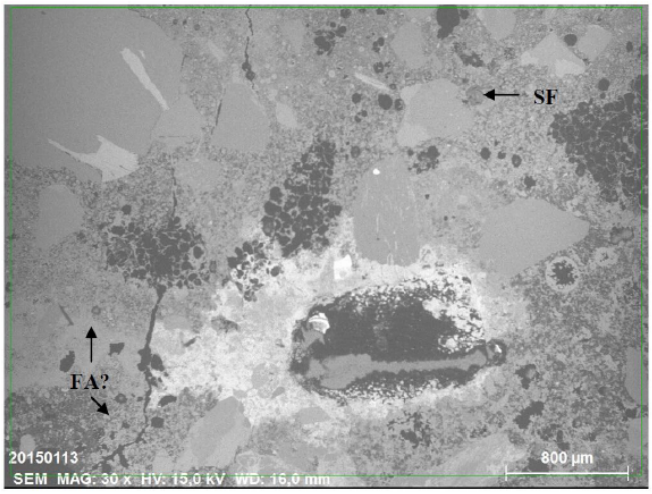

Figure 3: Back scatter image of severely carbonated perlite concrete (thin section N2) with Fe-rich corrosion product (bright) having stained adjacent carbonated cement paste matrix. Aggregate particles were mainly sand consisting of quartzite with biotite (upper left), pure quartz and granitic rocks. Undispersed silica fume (SF) and suspect fly ash (FA?) occurred. The dark areas are pores in extruded perlite and air voids, and a hole in the thin section due to a lost corroded steel fiber (cf. Figure 4).

with precipitates of calcium carbonate, representing a local weakness zone near the perlite concrete layer. However, grey friable micro-PP fiber concrete, represented by sample Nes-3, clearly showed that also parts of the outer concrete was partly severely attacked, as shown in Figure 8.

Chemical analysis of thin sections N1 and N2. Table 4 summarises the EDS analyses performed on the thin sections. Most of the analysed points and frames are shown in Figures 5 and 6. The carbonates were represented by three forms; 1) PCD in the cement paste matrix, 2) deposits on air voids in paste ("Cc" in Table 4) and within perlite and 3) very fine grained carbonation resembling ordinary carbonation due to atmospheric CO_2. The finer carbonation was not analysed.

The chemical composition of *perlite glass* was similar to rhyolite: In terms of oxide components (weight percent), the analysis N1-7 (Figure 7A) corresponds to: Na_2O = 4.08 %, K_2O = 4.56 %, Al_2O_3 = 13.69 %, SiO_2 = 74.63% and CaO = 3.04 %. The apparent absence of iron and magnesium is typical of a source material, which represents highly differentiated late stage volcanic melts. No sulfur was detected in extruded perlite glass. N1-8 represents apparent non-degraded CSH-rich paste sitting within a pore in a big perlite aggregate. Carbon and sulfur were not detected. In contrast analysis N1-5 from cement paste among PCD in presence of collapsed perlite, showed a very severe Ca-depletion, which is a typical feature of PCD concrete (Sibbick et al. 2003, Hagelia and Sibbick 2009). The depleted paste was otherwise apparently carbonated and sulfurised.

The PCD compositions and calcium carbonate deposits were not pure calcite. They were substituted by a small amount of magnesium, and were also sulfurised. Smaller amounts of alkalis, aluminium and silicium also occur, which may be chemically bound to the carbonates. The C/Ca+Mg –atomic ratio in calcite is 1. However, apart from a very low ratio of 0.33 in N1-3, the ratios in PCD and calcium carbonate deposits varied from 0.53 to 0.72 (cf. Figures 5 and 6). The C/Ca+Mg–ratio in carbonate analysis N2-4 (cf. Figure 6B) was 0.53, which is very close to 0.5 in $Ca(HCO_3)_2$. Hence PCD and the other carbonate deposits were apparently a mixture of calcite and calcium bicarbonate, although amorphous calcium carbonate (ACC) might not be ruled out. Also N1-6 (rust) of a thick corrosion product after steel fiber apparently contained an iron-carbonate component.

The thaumasite–like phases (N2-3 and N2-5), had an odd composition with unusually high carbonate contents. The Si/Al ratios were about 2 indicating intergrowth of thaumasite and ettringite. The Ca/Si+Al ratios were 1.02 and 1.4 and the Ca/S ratios were 2.0 to 3.8 as opposed to thaumasite and ettringite ratios, being equal to 3 for both ratios in both minerals. The mineral resembles aspects of $Ca_6Al_3(CO_3)_3(OH)_{12} \cdot 26H_2O$ (carbonate ettringite). However, in the present case Si substituted for Al and carbonate might have substituted for some of the OH^- groups.

The silica fume lump (N2-2) had a surprisingly low Si and unexpected high Mg. SiO_2 in silica fumes are usually well above 80 wt. %, whilst the Si atomic % in Table 4 corresponds to SiO_2 =

Erratum: Correct atomic ratio: Ca+Mg/C (not C/Ca+Mg)

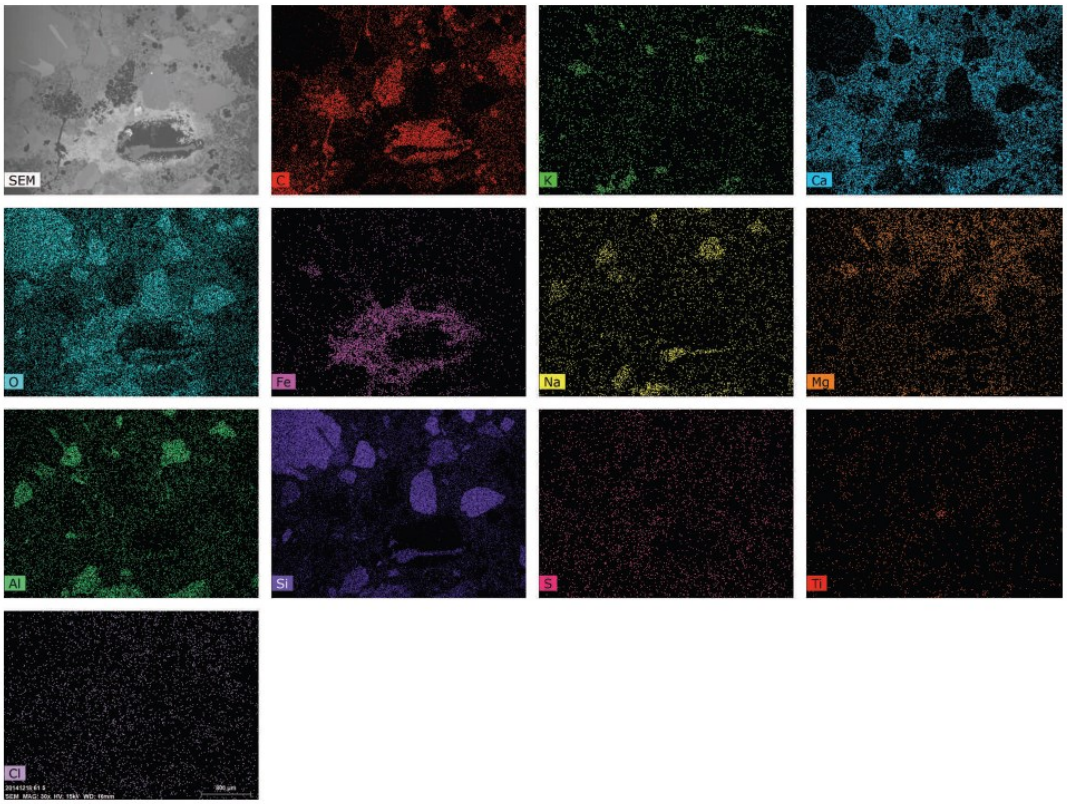

Figure 4: X-ray map of the domain shown in Figure 3. High carbon intensities within perlite and corrosion product represent the epoxy used in thin section preparation, whilst lower C intensities represent calcium carbonate. High K, Na, Al and Si represent aggregate. The cement paste matrix was extensively carbonated (Ca) containing a little S, reflecting variably Mg substituted calcium carbonate phases. Na and Cl were scattered about at fairly low concentrations in the matrix.

22.97 wt. %. The composition of brown mainly unreacted transparent glass sphere (N2-23) corresponded quite well with Type C fly ash. CaO in the analysed particle is 22.64 wt. %. Type C fly ash is not a highly pozzolanic material.

Small samples. The analysed domains were chosen from thick areas and single phases such that possible influence from the carbon tape should be

Table 4: SEM – EDS analysis of thin sections N1 (carbonated perlite concrete) and N2. All samples were from extensively degraded perlite concrete; except for adjacent micro-PP fiber concrete N2-3 through N2-5. *All data in atomic %.*

	N1-3 PCD	N1-4 PCD	N1-5 Paste	N1 Cc	N1-6 Rust	N1-7 Perlite	N1-8 CSH	N2-1 Cc	N2-2 SF	*N2-3 T-E**	*N2-4 Cc**	*N2-5 T-E**	N2-23 FA?	N2-24 PCD
C	23.64	20.29	29.72	20.98	14.34	0.00	0.00	21.75	21.36	30.45	19.53	27.94	16.52	22.55
O	63.37	61.63	65.86	60.80	59.26	63.01	60.27	61.39	64.03	65.35	62.30	64.50	62.23	61.93
Na	0.40	0.45	0.29	0.58	0.00	2.72	1.31	0.66	0.45	0.34	0.85	0.36	1.02	0.00
Mg	0.49	0.50	0.16	0.40	0.00	0.00	3.07	0.27	4.31	0.00	0.45	0.20	0.67	0.10
Al	0.77	0.73	0.47	0.31	1.61	5.54	4.19	0.29	0.98	0.46	1.24	0.36	2.72	0.29
Si	3.23	3.18	2.01	1.03	3.37	25.61	20.13	1.50	6.52	1.02	5.03	2.04	7.35	0.65
S	0.13	0.13	0.03	0.22	0.00	0.00	0.00	0.29	0.02	0.76	0.06	0.89	0.00	0.26
Cl	0.00	0.00	0.00	0.00	0.00	0.00	0.31	0.00	0.06	0.05	0.04	0.08	0.00	0.00
K	0.36	0.44	0.17	0.09	0.00	2.00	1.45	0.00	0.00	0.06	0.13	0.05	0.50	0.00
Ca	7.40	12.47	1.23	14.78	1.00	1.12	8.26	13.85	1.90	1.51	9.99	3.38	7.73	14.23
Fe	0.21	0.20	0.06	0.79	20.42	0.00	1.01	0.00	0.37	0.00	0.38	0.21	1.28	0.00

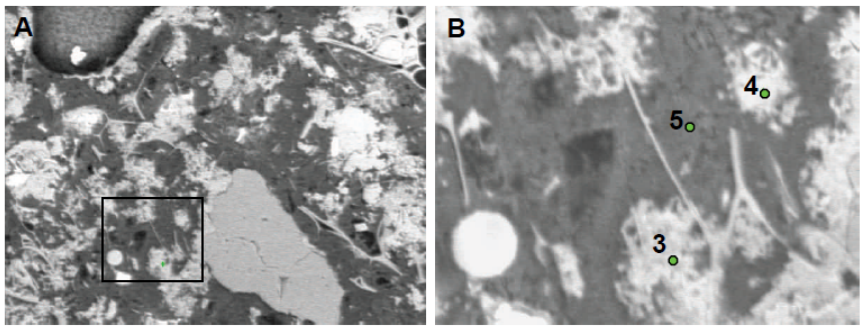

Figure 5: Thin section N1 of severely leached perlite concrete (Back Scatter). A: Dark grey = depleted cement paste, Light colored irregular = Popcorn calcite deposits (PCD); Light colored strings = broken up and collapsed perlite. The aggregate to the right of inset image is quartz. Width of field = 300 µm: B: Detail with analytical points, with numbers corresponding to Table 4. Width of field = 75 µm.

kept at a minimum. In contrast to the thin sections, sodium was detected in all analysis (Table 5). The analysed areas and points are indicated in Figure 7, being less accurate than the thin section analyses.

Sample Nes 1 of thenardite-rich white powder of completely degraded perlite concrete was analysed as bulk and in two individual grains. The bulk analysis (Nes 1a), representing an about 0.35 mm x 0.4 mm area centered on Figure 7A, showed very low Si, being much lower than the quartz content by XRD would seem to indicate. Moreover, the Na and S concentrations (7.24 and 2.60 atom %) were lower than expected for this thenardite rich material. Thus, the sample is not exactly the same as the one used for XRD, despite taken from the same small batch. However the Na/S ratio was near that of thenardite. The bulk analysis also indicated high contents of C and O, indicating presence of carbonate, with possible interference with the carbon tape. The point analyses of thenardite –like single crystals (Nes 1b and Nes 1c) showed that ratios of Na, S and O are compatible with thenardite. In contrast point analysis Nes 1c had no C despite sitting next to the former thenardite with C, suggesting that C variation is real. Minor amounts of Si, Al and Ca may represent very fine debris. Cl and Mg were absent.

Sample Nes 2 representing white degraded and very friable perlite concrete was analysed in three points. Nes 2b is an acicular phase quite similar to CSH, yet with much S and Na. The Na/S ratio was higher than ordinary sodium sulfate. Nes 2c is a point analysis in fine grained material, perhaps reflecting the composition of more than one phase. Yet, the Na/S ratio was very high due to low S, suggesting Na is not just restricted to sodium sulfate. Nes 2d of a single grain has a Na/S ratio being compatible with thenardite. It should further be noted that Nes 2 and especially point 2c contained Cl, likely derived from de-icing salts. Mg was also detected here.

Sample Nes 3 represents a small sample collected from grey friable micro-PP fiber concrete. Nes 3a is a point analysis of a tiny grain, which may reflect other near by grains. The analysis is somewhat comparable with bulk analysis of the entire frame of Figure 7C (3b), reflecting a mixture of CSH-like phases and sodium sulfate. However, also in this case the high Na/S ratios suggest excess Na. Point Nes 3c reflects an outer thin deposit of Na and S bearing material with Na/S ratio similar to thenardite, sitting on a substrate of CSH-like material. Also 3d resembles a mixture of thenardite and CSH. The Ca/Si ratios in friable micro-PP concrete do not indicate extensive Ca-depletion. A little Cl and Mg were also present. Figure 8, which encompass Figure 7D, shows that this concrete was extensively influenced by degradation in presence of sodium sulfate.

The general impression of the debris samples was that sodium sulfate is omnipresent and disseminated within CSH-like phases. Sodium also seems to be in excess in comparison with thenardite.

Sulfur isotopes

Sulfur isotopes were analysed in order to put constraints on possible sulfur sources. The thenardite-rich sample Nes-1 and sample N1 with extensive carbonation by sulfurised PCD and partly collapsed perlite within Ca-depleted cement paste matrix were selected. The relatively heaviest sulfate was detected in bulk analysis of N1 ($\delta^{34}S$ = +9.19 ‰), whilst sulfate in thenardite and sulfate in bulk residue of N1 after acid leaching were lighter ($\delta^{34}S$ = +7.44 ‰ and $\delta^{34}S$ = +5.73 ‰, respectively). The standard NBS 127 was run as unknown, yielding $\delta^{34}S$ = +21.60 ‰, which is 0.50 ‰ higher than the true value. The data allow us to calculate the isotopic composition of sulfur in the carbonates, on the likely assumption that sulfur isotopes behaved

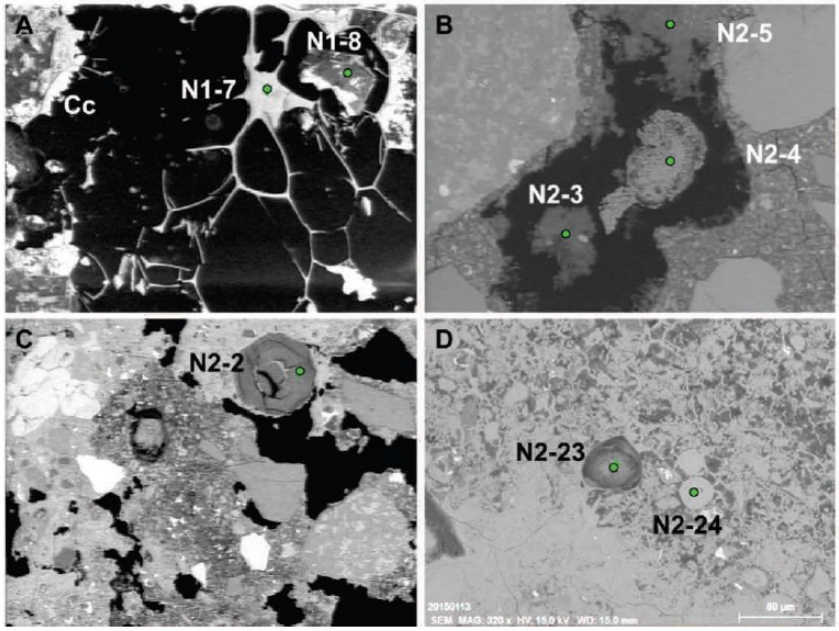

Figure 6: Back scatter images of thin sections N1 and N2. A: Close up of perlite showing analytical points on glass (N1-7) with fragment of CSH-like paste (N1-8) and calcite (Cc) precipitate inside perlite (width of field = 350 µm). B: Carbon-rich thaumasite-ettringite phases (N2-3 and N2-5) and $Ca(HCO_3)_2$ (N2-4) (width of field = 350 µm). C: Undispersed silica fume (N2-2) within outer porous micro-PP fiber concrete (width of field = 780 µm). D: Extensively carbonated perlite concrete with suspect fly ash (N2-23) and circular PCD (width of field = 400 µm).

as a conservative mixture. Thus, accounting for the mix proportions of bulk and residue of sample N1, sulfurised PCD and associated carbonate and possibly other soluble sulfate yielded $\delta^{34}S$ = +9.57 ‰. However, in view of the results from NBS 127, the real values should be about 0.5 ‰ lighter in all samples. The lightest S isotopic composition in the residue represents refractory sulfur sitting within less soluble material in perlite concrete, possibly involving depleted paste and perlite. The intermediate composition of thenardite sulfur suggests influence from two different sources.

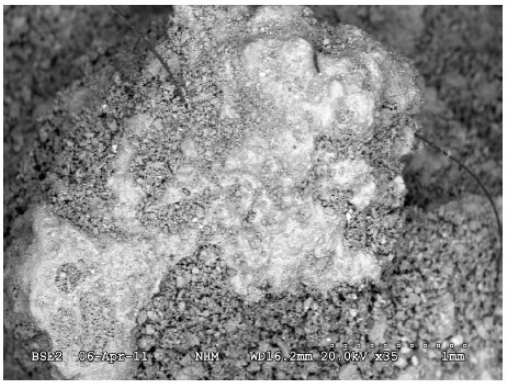

Figure 8: Sample Nes 3 of micro-PP fiber concrete showing significant degradation due to sodium sulfate and carbonation.

IV. Discussion

This paper has shown that the exceptional degree of spalling and steel fiber corrosion within sprayed concrete for fire protection in the Nes road tunnel was intimately associated with severe Ca-depletion and extensive carbonation under significant influence of sodium sulfates. The present discussion focuses on the causes, mechanisms and the sources of aggressives, as high-lighted by the overall context of the tunnel concrete. The tunnel environment here was characterised by variable moisture loads, frost action and heavy traffic under influence of deicing salts, being dependent on seasonal variations. The fact that spalling in the perlite concrete had led to repair work already in 2002 and that spalling in both new and old perlite concrete continued, having caused weakening also in adjacent new outer micro-PP concrete without perlite, seems to suggest that the degrading agents/mechanisms were acting over a long time. This needs to be explained.

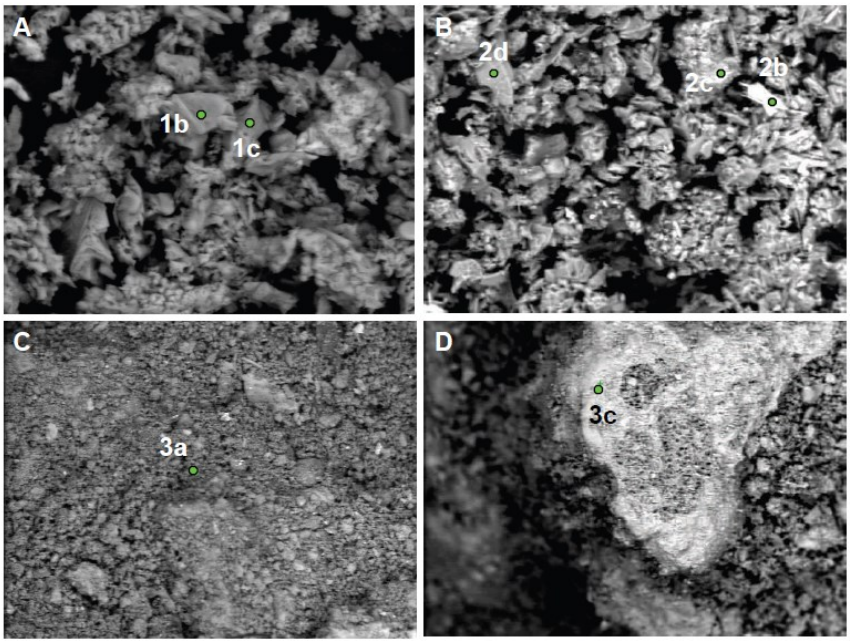

Figure 7: BSE images of selected domains in small samples. The analytical results are presented in Table 5. A: Sample Nes 1 (perlite concrete) with analysed points 1b and 1c; Image width = 250 µm. B: Sample Nes 2 (perlite concrete) with analysed points 2b, 2c and 2d; Image width = 250 µm. C: Sample Nes 3 (micro-PP fiber concrete) with analysed point 3a. Analysis 3b represents a bulk scan over the entire frame; Image width = 410 µm. D: Nes 3 with point 3c. Image width = 200 µm.

Formation conditions for sodium sulfate

Due to the severe Ca-depletion of CSH involving capture of Ca in calcite and calcium bicarbonate, formation of gypsum and thaumasite in presence of sulfate ions should be strongly inhibited. Thus, when significant Na and sulfate is present, thenardite and other sodium sulfates may form. This has also been observed in some Austrian tunnels, where mirabilite formed at a very late stage after thaumasite sulfate attack (Mittermayr 2012). Hence, in such contexts internal carbonation is a prerequisite for later stage formation of sodium sulfate. Water glass used as setting accelerator was likely a main source of sodium, although de-icing salt likely also contributed. This would explain some evidence of excess Na relative to sulfur. Before turning to the discussion of possible sulfate sources we need to explain the mechanisms causing severe Ca-depletion and internal carbonation.

Mechanism of Ca-leaching and carbonation

Ca-leaching was omnipresent in the perlite concrete with ubiquitous presence of Popcorn calcite deposition (PCD) with additional very fine grained carbonation. The PCD form of carbonation is commonly observed in submerged concretes structures, such as tunnel sprayed concrete for rock support in black shale and subsea environments (Hagelia et al. 2001; Hagelia et al. 2003, Hagelia 2011); in cast concrete involving seawater attack in brackish water (Sibbick et al. 2003a & b) and concrete in sewage systems (Fernandes et al. 2012). PCD is frequently associated with thaumasite sulfate attack and sulfuric acid attack, but may also take place in absence of sulfate, e.g. in through solution processes with ingress of a carbonate source, such as bicarbonate (Gaze and Crammond 2000; Hagelia et al. 2001; Sibbick et al. 2003). PCD is generally regarded as a form of carbonation which may lead to significant weakening of the cement paste matrix, involving increased water permeability and steel reinforcement corrosion. This stands in marked contrast to ordinary surface carbonation, being mainly harmful to steel reinforcement.

Van der Sloot (2000) reported that Ca is much more leachable than Si, being about 90-95 % and 0.015 % respectively. Obviously, these figures are manifested in concretes which have suffered Popcorn calcite deposition, e.g. where ingress of external bicarbonate-bearing water with a neutral pH meets the alkaline cement pore fluids, causing entrapment of leached Ca in secondary calcite, leaving behind a substrate mainly consisting of amorphous silica and other less mobile elements.

The analytical data from the Nes tunnel showed

Table 5: SEM – EDS analysis. All samples were from extensively degraded perlite concrete, except for Nes-3 of micro-PP fiber concrete. *The micro domains are shown in Figure 7 (except 3d).*

	Nes 1a Bulk paste	Nes 1 b Na-sulf	Nes 1 c Na-sulf	Nes 2b Single	Nes 2c mixed	Nes 2d Single	*Nes 3a Paste*	*Nes 3b Bulk paste*	*Nes 3c mixed*	*Nes 3d mixed*
C	28.47	19.94	0.00	7.62	11.07	10.98	14.29	22.66	17.23	19.28
O	61.03	49.44	24.43	51.61	46.36	51.4	59.99	62.00	55.81	60.44
Na	7.24	18.40	46.06	12.22	21.58	17.71	4.46	1.81	8.30	4.27
Mg	0.00	0.00	0.00	0.37	0.68	0.4	0.89	0.54	1.12	0.63
Al	0.04	0.02	0.23	1.69	1.38	1.61	2.31	0.56	0.82	1.45
Si	0.13	0.11	0.42	6.74	3.76	7.65	8.95	2.03	2.51	5.61
S	2.60	11.97	28.59	3.84	1.52	7.53	0.68	0.20	4.09	1.43
Cl	0.00	0.00	0.00	1.73	10.35	0.23	1.22	0.36	0.28	0.64
K	0.00	0.00	0.00	0.63	0.28	0.03	0.72	0.22	0.00	0.39
Ca	0.12	0.13	0.33	7.26	2.34	1.34	5.88	8.83	9.47	5.73
Fe	0.00	0.00	0.00	6.30	0.68	1.03	0.54	0.19	0.38	0.00
Ti	0.00	0.00	0.00	0.00	0.00	0.00	0.08	0.60	0.00	0.12
F	0.35	0.00	0.00	0.00	0.00	0.00	0.00	0.00	0.00	0.00

that PCD and associated calcium carbonate precipitates were not pure calcite. Instead they apparently represent a mixture of calcium carbonate and calcium bicarbonate ($Ca(HCO_3)_2$) and were otherwise sulfurised, substituted by Mg and also contained a little K, Na, Al and Si. Standard chemical literature states that calcium carbonate dissolves in excess of CO_2 to form calcium $Ca(HCO_3)_2$. It is interesting that the XRD of small samples did not record a lot of calcite as opposed to what was indicated by generally elevated C and O in the SEM-data. Hence, it seems possible that these carbonates in fact may represent some form of amorphous calcium carbonate (ACC).

In the Nes tunnel, it seems evident that bicarbonate was present in the ground water, due to the occurrence of thermonatrite efflorescence on the rock mass. However, spalling had occurred all over the place, and was not restricted to water seeping through joints in the PE-foam panels. Hence we mainly need to invoke atmospheric CO_2 as the likely main source of carbonate, which when dissolving into water forms carbonate ions when pH is much alkaline, and bicarbonate at circum-neutral pH. Nevertheless, this cannot explain why severe Ca-depletion was brought about. Indeed, such a reaction is most typically associated with influence of acidic waters, as was also suggested by the petrographic features.

Origin of thenardite sulfate

No report suggests significant concentrations of sulfate in the local ground water. There is no industry in the area, and the rock mass is completely dominated by rhomb porphyry which has a feldspar-rich mineralogy with composition similar to latite. Most of the spalling concrete was also screened from external water by still intact PE-foam plates. Hence, it must be concluded that the sulfate originated from the sprayed perlite concrete itself.

The S isotopic data showed that thenardite sulfur must reflect two different sources. Possible sources are the gypsum added to the cement and perlite, because the concrete aggregate did not contain any sulfur bearing mineral. The heaviest sulfur was sitting in the sulfurised carbonates (calculated to $\delta^{34}S$ = +9.57 ‰), whilst the lightest was sitting in residue after acid leaching ($\delta^{34}S$ = +5.73 ‰). For comparison, previous analysis of fairly intact CSH in thaumasite bearing Norwegian sprayed concrete were ranging from $\delta^{34}S$ = +10.6 ‰ to $\delta^{34}S$ = +11.8 ‰. These concretes were made in 1987 and 1999, respectively, and their S isotopic compositions were interpreted to largely reflect gypsum added to the cements (Iden and Hagelia 2003). However, associated thaumasite derived from external sulfate had

Table 6: S isotopic signatures of sulfates in thenardite; bulk carbonated concrete and residue after acid leaching.

Sample No.	Sample type	$\delta^{34}S_{CDT}$ (‰)	S (Wt. %)
Nes-1	Powder rich in thenardite with some quartz	+7.44	-
N 1	Bulk of extensively carbonated concrete	+9.19	0.10
N 1	Residue after washing with 2M HCl	+5.73	0.01
NBS 127	Standard with true value $\delta^{34}S_{CDT}$ = 21.1‰	+21.60	

$\delta^{34}S \approx +2$ ‰, which hints that the composition of added gypsum might have been slightly heavier than about 11-12 ‰.

It should be noted that gypsum sources used in cement production are represented by ancient evaporites, having distinct age- dependant S isotopic signatures. This depends on the isotopic variations in the ancient seas from which gypsum evaporated. The lightest possible S isotopic signatures of significant gypsum deposits are represented by uppermost Permian to lowermost Triassic evaporites, being $\delta^{34}S \approx +10$-13 ‰(Claypool et al. 1980). Data from Zechstein anhydrite units in West Poland have $\delta^{34}S = +9.6$ ‰to +12.6 ‰(Peryt el al. 2010). On the other hand other sources of gypsum with heavier sulfur are possible. Unpublished data of the author from Norwegian cement shows that gypsum with $\delta^{34}S = +21.3$ ‰has been used just after year 2000. However, there are reasons to believe that the Nes tunnel was made with cements from the same factory as our previously investigated sprayed concretes, being constructed at more or less the same time. Hence, it may be concluded that all of the S isotopic signatures obtained from the Nes tunnel are significantly lower than the minimum estimate for added gypsum ($\delta^{34}S \approx +11$-12 ‰): The $\delta^{34}S$ compositions obtained in a) sulfurised carbonate (PCD), b) thenardite and c) the residue after acid leaching are about 2 ‰, 4 ‰and 6 ‰lighter than any possible gypsum source, respectively. All compositions may be regarded as intermediate between two sulfur sources. It is implicit that the heavier end-member must be represented by added gypsum, whilst the lighter end-member clearly seems represented by sulfuric acid.

The lighter sulfate source involved was bound to the less soluble phases in the Nes carbonated perlite concrete. It is therefore quite possible that this is represented by SO_2 gas initially trapped within the pore space of extruded perlite. In the first place SO_2 must be expected to have been present in the perlite raw material, being a common volcanic gas. Moreover, during the production of extruded perlite this gas can be trapped in the pore space if oil or coal has been used for combustion. However, for the extruded perlite used in the Nes tunnel, no chemical documentation is available.

The main point here is that sulfur dioxide has a very light S isotopic composition, frequently showing negative $\delta^{34}S$ signatures (Faure 1986), and that it reacts with water to form sulfuric acid. In view of the observation that the pore space of perlite had frequently collapsed during the spraying operation (Figure 5B) this should indeed facilitate direct access to any possible aggressive gas at the earliest stage, likely before and during early setting of the cement. If so, it would seem likely that cement hydration never went well, and that portlandite perhaps never formed. This may also explain why sulfur was distributed evenly throughout the cement paste matrix as seen in Figure 4. This is not at odds with the fact that the perlite glass was sulfur free. It is, however, not possible to put further constraints on the amount of sulfuric acid involved, because we do not explicitly know whether the added gypsum sulfur was similar to Zechstein or even heavier.

Reaction mechanisms

The fact that thenardite (type V) and sodium sulfate (type III) occurred in the main spalling zone shows that salt crystallisation represented an important ingredient in the spalling process. It was argued above that Ca-leaching assisted by sulfuric acid derived from perlite, with PCD acting as a sink for liberated calcium was a prerequisite for the formation of sodium sulfate. Yet, the sprayed concrete used for fire protection in the Nes tunnel had clearly been influenced by frost and also variable moisture loads in presence of de-icing salts, depending on seasonal variation. Moreover, this kind of tunnel lining is sensitive to pressure waves from traffic, because the construction is pretty slim and mounted to the rock mass by bolts. The thin concrete layers outside foam panels has in fact been subjected to dynamic loads, which must have resulted in microcracking at an increasing rate, hence making the concrete more and more susceptible to degradation by combined freeze/thaw, salt crystallisation and dissolution.

The relative humidity (RH) in Norwegian tunnels is generally < 60 %. For this reason it is of no surprise that mirabilite was not detected, since this mineral is only stable at RH > 65 % for Norwegian tunnel temperatures. Until recently the conversion of thenardite to mirabilite has been regarded as most important for build-up of crystallisation pressure and spalling (Skalny et al 2002), owing to their great differences in molar volume ($V_{thenardite}$ = 53.30 cm^3/mol versus $V_{mirabilite}$ = 218.56 cm^3/mol). However, research has shown that the effects of thenardite have been underestimated. This is due to more complex phase changes, along with the significant impact from degree of supersaturation. Indeed, the growth pressure of thenardite may be about four times higher than that of mirabilite at high supersaturation. Cyclic conversion tests have demonstrated that thenardite alone can inflict considerable damage to rocks of different porosities (Yu and Oguchi 2013). Rodriguez-Navarro et al (2000) reported that fast evaporation due to lowering of RH conditions, leading to high supersaturation in micropores before thenardite precipitation, results in high crystallisation pressure of thenardite, whilst mirabilite crystallises at lower level of supersatura-

Note added: Interestingly, mordenite was detected in friable sample Nes-2, similar to N1. This zeolite has a high capacity to adsorb SO_2 (Stenger et al. 1993).

tion generally as efflorescence.

Due to the extensive presence of weak and powder-like concrete it is likely that mass transfer during freezing in the spalling region might be compared to mechanisms taking place within saline soils. Chuvilin et al. (1998) have demonstrated that water soluble salts such as sodium sulfate have a fundamental influence on the process of ice formation and the formation of cryogenic structures. They reported that the mass transfer of salt in freezing saline soils is a result of ion transfer within the water flux, surface conduction, diffusion and thermodiffusion; the most important process is the transfer of salt ions within the water flux. The maximum accumulation of water corresponded to the largest accumulation of salt, hence being prone to supersaturation of thenardite.

V. Conclusions

The Nes road tunnel was closed for nearly three years due to extensive spalling of perlite concrete used for fire protection. The present investigation has shown that the degradation process began with early stage leaching of the cement paste matrix, due at least in part to involvement of sulfuric acid derived from sulfur dioxide gas in the perlite pore space. PCD and other carbonates formed a sink for Ca, which consequently made way for sodium sulfate formation with significant and repeated salt crystallisation/dissolution events taking place within the main spalling zone. During winter salt scaling was acting in harmony with the freeze/thaw cycles. The effects of dynamic loads from traffic accentuated the speed of the attack.

Acknowledgements

The author is deeply indebted to mineralogist and analyst Hans-Jørgen Berg († 2014) of the Natural History Museum (NHM), Oslo, for technical assistance with XRD and SEM, and not the least for his knowledge and insight, which he always shared with us with the greatest dedication. I also acknowledge technical assistance by Harald Folvik NHM and skillful preparation of thin sections by Salahadin Akhavan at the University of Oslo. Ingar Johansen and Christian Alexander Schöpke at Institute for energy technology, Kjeller, deserve thanks for doing the isotope analysis. Lastly the author wishes to thank Synnøve Myren at the Norwegian Public Roads Administration for assistance and for digging up important information. This report was prepared for the R&D project "Durable structures" at NPRA.

References

Chuvilin, E.M., Ershov, E.D. and Naletova, N.S. (1998): "Mass transfer and structure formation in freezing saline soils." Permafrost - Proceedings of 7th International Conference, Yellowknife, Canada, *Collection Nordicana*, No 55, 173-179.

Claypool, G.E., Holster, W.T., Kaplan, I.R. Sakai, H. and Zak, I. (1980): "The age curve of sulfur and oxygen isotopes in marine sulfate and their mutual interpretation". *Chemical Geology*, 28, 199-260.

Davik, K.I. (1998): "Proper use of sprayed concrete". *Nordic Road and Transport Research*, 1998-1, 16-17.

Fernandes, I., Pericão, M., Hagelia, P. Noronha, F., Ribeiro, M.A. and Maia, J. (2012): " Identification of acid attack on concrete of a sewage system". *Materials and Structures*, 45-3, 337-350.

Faure, G. (1986): "Principles of Isotope Geochemistry". (2nd Ed.). John Wiley and Sons, 589 p.

Gaze, M.E. and Crammond, N.J. "The formation of thaumasite in a cement, lime, sand mortar exposed to cold magnesium and potassium sulfate solutions". *Cement and Concrete Composites*, 22, 209-222.

Hagelia, P. (2007): "Sprayed concrete deterioration influenced by saline ground waters and Mn-Fe biomineralisation in subsea tunnels". In: B. Jamtveit (Ed), *Mechanical Effects on Reactive Systems, the 20th Kongsberg Seminar*, 2007, p 26 (abstract).

Hagelia, P. (2011): "Deterioration Mechanisms and Durability of Sprayed Concrete for Rock Support in Tunnels" PhD thesis, TU-Delft, 205 pp and Appendices.

Hagelia, P. (2013): "Interaction of abiotic and biochemical reactions and their role in concrete deterioration". *Concrete*, July/August, 49-51.

Hagelia, P., Sibbick, R.G., Crammond, N.J., Grønhaug, A.W. and Larsen, C.K. (2001): "Thaumasite and subsequent secondary calcite deposition in sprayed concrete in contact with sulfate bearing Alum Shale, Oslo, Norway". *8th Euroseminar on Microscopy Applied to Building Materials*, Athens, Greece, 131-138.

Hagelia, P., Sibbick, R.G., Crammond, N.J. and Larsen, C.K. (2003): "Thaumasite and secondary calcite in some Norwegian concretes". *Cement and Concrete Composites*, 25, 1131-1140.

Hagelia, P. and Sibbick, R.G. (2009): "Thaumasite sulfate attack, popcorn calcite deposition and acid attack in concrete stored at the Blindtarmen test site Oslo, from 1952 to 1982." *Materials Characterisation*, 60, 686-699.

Stenger, H. G., Hu, K., & Simpson, D. R. (1993). Competitive adsorption of NO, SO_2 and H_2O onto mordenite synthesized from perlite. Gas separation & purification, 7(1), 19-25.

Holm, J.V. (2011): "E16 Nestunnelen – nedfall av sprøytebetong". Norconsult - Notat nr.1, Oppdragsnr. 5111160.

Iden, K.I. and Hagelia, P. (2003): "C, O and S isotopic signatures in concrete which have suffered thaumasite formation and limited thaumasite form of sulfate attack". *Cement and Concrete Composites*, 25, 839-846.

Mittermayr, F. (2012): "Why thaumasite is forming in concrete structures". PhD thesis, TU-Graz, 119 pp.

Norwegian Public Roads Administration (1997): "Proper use of sprayed concrete in tunnels". Parts A, B, C, D, E and Final report (In Norwegian).

Peryt, T.M., Hałas, S. and Hryniv, S.P. (2010): "Sulphur and oxygen isotope signatures of late Permian Zechstein anhydrites, West Poland: seawater evolution and diagenetic constraints". *Geological Quarterly*, 54(4), 387-400.

Rodriguez-Navarro, C., Doehne, E. and Sebastian, E. (2000): "How does sodium sulfate crystallise? Implications for the decay and testing of building materials". *Cement and Concrete Research*, 30, 1527-1534.

Sibbick, R.G., Crammond, N.J. and Metcalf, D. (2003a): "The microscopical characteristics of thaumasite." *Cement and Concrete Composites*, 25, 831-837.

Sibbick, R.G., Fenn, D. and Crammond, N.J. (2003): "The occurrence of thaumasite as a product of seawater attack". *Cement and Concrete Composites*, 25, 1050-1066.

Skalny, J.P., Marchand J., Odler I. (2002): "Sulfate Attack on Concrete". Modern Concrete Technology Series 10, Spon Press – Taylor and Francis Group, London and New York

Van der Sloot, H.A. (2000) "Comparison of the characteristic leaching behaviour of cements using standard (EN 196-1) cement mortars and an assessment of their long-term environmental behaviour in construction products during service life and recycling". *Cement and Concrete Research*, 30-7 1079-1096.

Yu, S. and Oguchi, C.T. (2013): "Is sheer thenardite attack impotent compared with cyclic conversion of thenardite-mirabilite mechanism in laboratory simulation tests?" *Engineering Geology*, 152, 148-154.

Statens vegvesen
Vegdirektoratet
Publikasjonsekspedisjonen
Postboks 8142 Dep 0033 OSLO
Tlf: (+47 915) 02030
publvd@vegvesen.no

ISSN: 1893-1162

vegvesen.no

Trygt fram saman